

Greenhouse gas fluxes over managed grasslands in Central Europe

Lukas Hörtnagl, M Barthel, N Buchmann, W Eugster, K Butterbach-Bahl, Eugenio Díaz-Pinés, M. Zeeman, Katja Klumpp, Ralf Kiese, M Bahn, et al.

► To cite this version:

Lukas Hörtnagl, M Barthel, N Buchmann, W Eugster, K Butterbach-Bahl, et al.. Greenhouse gas fluxes over managed grasslands in Central Europe. Global Change Biology, 2018, 24 (5), 10.1111/gcb.14079. hal-01714760

HAL Id: hal-01714760 https://hal.science/hal-01714760

Submitted on 21 Feb 2018

HAL is a multi-disciplinary open access archive for the deposit and dissemination of scientific research documents, whether they are published or not. The documents may come from teaching and research institutions in France or abroad, or from public or private research centers.

L'archive ouverte pluridisciplinaire **HAL**, est destinée au dépôt et à la diffusion de documents scientifiques de niveau recherche, publiés ou non, émanant des établissements d'enseignement et de recherche français ou étrangers, des laboratoires publics ou privés.



Distributed under a Creative Commons Attribution - NonCommercial 4.0 International License

Article type : Primary Research Articles **Title page** Greenhouse gas fluxes over managed grasslands in Central Europe running head: GHG fluxes over managed European grasslands Hörtnagl L. (1), Barthel M. (1), Buchmann N. (1), Eugster W. (1), Butterbach-Bahl K. (2), Díaz-Pinés E. (2,3), Zeeman M. (2), Klumpp K. (4), Kiese R. (2), Bahn M. (5), Hammerle A. (5), Lu H. (2), Ladreiter-Knauss T. (5), Burri S.(1) and Merbold L. (1,6) (1) ETH Zürich, Institute of Agricultural Sciences, Zürich, Switzerland, (2) Karlsruhe Institute of Technology (KIT), Institute of Meteorology and Climate Research, Karlsruhe, Germany, (3) University of Natural Resources and Life Sciences (BOKU), Institute of Soil Research, Vienna, Austria, (4) INRA, Grassland Ecosystem Research, Clermont-Ferrand, France, (5) University of Innsbruck, Institute of Ecology, Innsbruck, Austria, (6) Mazingira Centre, International Livestock

DR. LUKAS HÖRTNAGL (Orcid ID : 0000-0002-5569-0761)

DR. RALF KIESE (Orcid ID : 0000-0002-2814-4888)

Research Institute (ILRI), Nairobi, Kenya

This article has been accepted for publication and undergone full peer review but has not been through the copyediting, typesetting, pagination and proofreading process, which may lead to differences between this version and the Version of Record. Please cite this article as doi: 10.1111/gcb.14079 This article is protected by copyright. All rights reserved. Corresponding author: Lukas Hörtnagl, email: lukas.hoertnagl@usys.ethz.ch, phone: +41 44 632 58 71

Keywords: nitrous oxide, methane, eddy covariance, chamber, fertilizer, emission factor, carbon dioxide, grazing, management, livestock

Type of paper: Primary Research Article

Abstract

Central European grasslands are characterized by a wide range of different management practices in close geographical proximity. Site-specific management strategies strongly affect the biosphere-atmosphere exchange of the three greenhouse gases (GHG) carbon dioxide (CO_2), nitrous oxide (N_2O) and methane (CH_4). The evaluation of environmental impacts at site level is challenging, because most *in-situ* measurements focus on the quantification of CO_2 exchange, while long-term N_2O and CH_4 flux measurements at ecosystem scale remain scarce.

Here, we synthesized ecosystem CO₂, N₂O and CH₄ fluxes from 14 managed grassland sites, quantified by eddy covariance or chamber techniques. We found that grasslands were on average a CO₂ sink (-1783 to -91 g CO₂ m⁻² yr⁻¹), but a N₂O source (18 – 638 g CO₂-eq. m⁻² yr⁻¹), and either a CH₄ sink or source (-9 to 488 g CO₂-eq. m⁻² yr⁻¹). The net GHG balance (NGB) of nine sites where measurements of all three GHGs were available was found between -2761 and -58 g CO₂-eq. m⁻² yr⁻¹, with N₂O and CH₄ emissions offsetting concurrent CO₂ uptake by on average $21 \pm 6\%$ across sites. The only positive NGB was found for one site during a restoration year with ploughing. The predictive power of soil parameters for N₂O and CH₄ fluxes was generally low and varied considerably within years. However, after site-specific data normalization we

identified environmental conditions that indicated enhanced GHG source/sink activity ('sweet spots') and gave a good prediction of normalized overall fluxes across sites. The application of animal slurry to grasslands increased N₂O and CH₄ emissions. The N₂O-N emission factor across sites was $1.8 \pm 0.5\%$, but varied considerably at site level among the years (0.1 – 8.6%). Although grassland management lead to increased N₂O and CH₄ emissions, the CO₂ sink strength was generally the most dominant component of the annual GHG budget.

Introduction

Central European grasslands are characterized by a wide range of different management practices, ranging from intensively managed lowland pastures and meadows to rather extensively managed high alpine grasslands (Gilmanov *et al.*, 2007; Bahn *et al.*, 2008; Wohlfahrt *et al.*, 2008a). Farming systems operate within their socio-economic and environmental boundaries, leading to management decisions that define type, frequency, timing and intensity of management events (Huber *et al.*, 2013, Huber *et al.*, 2014).

Grassland management-such as the amount and type of fertilizer applied, the frequency of cutting or the duration of grazing-strongly impacts the exchange of greenhouse gases (GHG), water and energy between the grassland ecosystem and the atmosphere and subsequently affects the biogeochemical cycling of carbon (C) and nitrogen (N) (Schulze *et al.*, 2009). Annual GHG budgets of grasslands, consisting of the three GHGs carbon dioxide (CO₂), nitrous oxide (N₂O) and methane (CH₄), are thus influenced directly by management (Lal, 2010; Gelfand *et al.*, 2011). The atmospheric concentrations of all three trace gases are still increasing at present, with anthropogenic activities being the major driver (IPCC, 2013). Both N₂O and CH₄ have high warming potentials, 298 (N₂O) and 34 (CH₄) times that of a corresponding mass of CO₂ emitted on a 100-year time horizon (IPCC, 2013). Agricultural grassland management activities are

closely connected to emissions of both non-CO₂ gases and to the uptake or emission of CO₂ (Tubiello *et al.*, 2015). Emissions of N₂O and CH₄ can contribute to an increase of the net GHG balance (NGB) of a grassland, offsetting concurrent CO₂ sequestration in terms of CO₂-equivalents (Liu & Greaver, 2009; Schulze *et al.*, 2009). This offset can be large and can even result in shifting a grassland from being a net GHG sink to a net source. The CO₂ sink strength as well as the N₂O and CH₄ source strengths of grasslands have been found to vary significantly across years and sites (Soussana *et al.*, 2007; Gilmanov *et al.*, 2010).

N₂O is produced by microbial activities in soils, mainly via nitrification and denitrification processes. N₂O can also be consumed by microbial processes such as denitrification, so that the net flux of N₂O observed at the soil surface is the result of simultaneously occurring production and consumption processes (Butterbach-Bahl *et al.*, 2013). The production of soil N_2O is controlled by various factors, such as soil water content, temperature, pH and the amount of available labile C and N (Holtan-Hartwig et al., 2002; Barnard et al., 2005; Prentice & Ri, 2008). N₂O production in soils is fueled by high N availability, which is mainly caused by the application of organic (solid manures or liquid slurries) and synthetic fertilizers to soils, but also due to the cultivation of legumes (Davidson, 2009; Fowler et al., 2009; Lüscher et al., 2014). For grasslands and meadows, additional N input might originate from livestock excreta (urine and faeces) (Galloway et al., 2003; Saggar et al., 2013; Paustian et al., 2016). Application of organic and inorganic fertilizers have been shown to result in soil N2O emission peaks, the magnitude of which depends on form, amount and timing of applied N as well as presence or absence of organic matter (Laville et al., 2011). Due to the high spatial and temporal variability of N₂O production, estimating national and sub-national emissions remains difficult and is associated with major uncertainties (Reay et al., 2012). The importance of soils as sinks for atmospheric

CH₄ is mainly produced by single-celled archaea (methanogens) that are found in anaerobic microsites in the soil, water-saturated zones with high C content and the rumen of ruminants (Baldocchi et al., 2012; Hiller et al., 2014). Methanogenesis is the end point of the anaerobic breakdown of organic matter (Whalen, 2005). In Europe, the vast majority of agricultural CH_4 emissions originates from enteric fermentation (77%), but a considerable amount is also released as a consequence of manure decomposition processes (9%) during manure management (FAOSTAT, 2017). High CH₄ emissions were correspondingly reported from regions with intensive agriculture and animal husbandry (Barnosky, 2008; Schulze et al., 2009; Frankenberg et al., 2011). The major global sinks for CH_4 are biological oxidation by aerobic and anaerobic methanotrophs at CH₄ production sites, and photochemical oxidation by hydroxyl radicals in the atmosphere (Tate, 2015). Aerobic soils constitute an additional CH₄ sink, with atmospheric CH₄ diffusing into the soil and being oxidized by methanotrophic bacteria (Dunfield, 2007; Dutaur & Verchot, 2007; Unteregelsbacher et al., 2013). In these well-aerated soils, observed net CH₄ uptake is also the consequence of CH₄ consumption (methanotrophy) being larger than the CH₄ production (methanogenesis) in the soil (Conrad, 2009). Oxidation rates are influenced by abiotic factors such as soil moisture and soil temperature, with changes in soil moisture accounting for most of the observed variability (Price et al., 2004; Tate, 2015).

In Europe, 21% of the terrestrial surface is currently dedicated to agriculture (FAOSTAT, 2017). Most agricultural land is used for arable crops (59%), followed by permanent meadows and pastures (38%) and permanent crops, e.g. vines and olive trees (3%). In 2014, European

agriculture contributed 11% to global total GHG emissions from agriculture (FAOSTAT, 2017). Total European N₂O emissions in terms of CO₂-equivalents have exceeded CH₄ emissions since 2011, with N₂O contributing 52% (CH₄: 48%) to total European GHG emissions in 2014 (FAOSTAT, 2017). Although CH₄ emissions from enteric fermentation constitute the largest single source of GHGs from agriculture in Europe (2014: 38%), aggregated N₂O emissions from agricultural soils comprise an even larger share (46%), mainly as a consequence of nitrification and denitrification processes driven by synthetic and organic fertilizer application to the agricultural land (Soussana *et al.*, 2007; FAOSTAT, 2017). Manure related N₂O and CH₄ emissions in Europe, comprising CH₄ and N₂O emissions from manure management along with N₂O emissions from organic fertilizer and manure from grazing animals that is left on pastures, account for 30% of the total agricultural GHG emissions (FAOSTAT, 2017).

The net ecosystem exchange of CO_2 is the most important constituent of the grassland C cycle. The role of the CO_2 flux for the GHG budget can become even more pronounced in grasslands, as such ecosystems are often limited by soil N availability, and N addition during fertilization increases the CO_2 sink more than the N₂O and CH₄ sources (Gomez-Casanovas *et al.*, 2016). Although the CO_2 flux in response to abiotic, biotic and management drivers was studied previously (e.g., Wohlfahrt *et al.*, 2008a; Peichl *et al.*, 2013), direct measurements (of one year or longer) of N₂O and CH₄ grassland fluxes in combination with CO₂ fluxes are still rare (Kroon *et al.*, 2010; Hörtnagl & Wohlfahrt, 2014; Merbold *et al.*, 2014).

The accurate quantification of the three GHGs CO_2 , N₂O and CH₄ is relevant for climate policy. Following the Paris Climate Agreement (UNFCCC, 2015), each signing partner country is requested to accurately report GHG emissions from different sectors, e.g. from agriculture, forestry and other land use (AFOLU). In addition, countries are required to identify potential

GHG mitigation options. However, long-term measurements of GHG emissions from grasslands, which are part of the AFOLU sector, remain scarce. *In-situ* data have the potential to adequately reflect the small-scale variability of GHG emissions at farm scale, needed to give specific mitigation recommendations to stakeholders. In addition, they provide the data basis for biogeochemical process model development and validation. Availability and continuity of such direct ecosystem GHG flux measurements is crucial for assessing the GHG reduction potential of different management strategies (Luyssaert *et al.*, 2014).

In this study, we examined the GHG emission intensity of meadows and pastures. To this end, we analyzed available GHG measurements of 14 differently managed grassland sites in Central Europe across different environmental settings. Our specific objectives were (1) to provide an overview of currently available *in-situ* GHG measurements over managed grasslands, (2) to test the applicability of soil temperature and water-filled pore space, two key parameters for soil biogeochemistry and widely available in combination with flux measurements, for the prediction of N₂O and CH₄ fluxes across grassland sites, (3) to quantify the impact of fertilizer application on observed N₂O and CH₄ emissions, and (4) to provide net GHG balances and N₂O-N emission factors for all sites by gap-filling direct measurements at ecosystem scale.

Materials and Methods

This synthesis paper investigated CO_2 , CH_4 and N_2O fluxes from ten Central European grasslands along an elevation gradient (Table 1). Four out of the ten grasslands (FR-LAQ, CH-FRU, DE-FEN, CH-CHA) were divided into two separate areas with different management, leading to 14 grassland sites in total. The research sites span an altitudinal gradient from 400 - 1978 m a.s.l in Central Europe, with mean annual temperatures (MAT) ranging between -1.4 and 9.1°C and mean annual precipitation (MAP) ranging between 852 and 1682 mm (Table 1). Sites included in this study, listed in altitudinal order from highest to lowest, were the extensively managed site CH-AWS (1978 m a.s.l.), the extensive pasture AT-STU-P (1870 m a.s.l.), the extensive meadow AT-STU-M (1820 m a.s.l.), the semi-natural grassland site Laqueuille that was divided into two adjacent paddocks with intensive (FR-LAQ-I) and extensive (FR-LAQ-E) management (1040 m a.s.l.), the subdivided mountain rangeland at Früebüel, which consisted of the intensively managed site CH-FRU-I and the extensive site CH-FRU-E (982 m a.s.l.), the intensively managed AT-NEU (970 m a.s.l.), the extensive meadow DE-GAP (734 m a.s.l.), Fendt with an intensively and extensively managed paddock (DE-FEN-I, DE-FEN-E, 600 m a.s.l.), and the intensive site Chamau, which was subdivided into two areas during a chamber measurement campaign in 2010 / 2011 (CH-CHA-II), while in 2012, CH₄ and N₂O fluxes were measured using the eddy covariance technique covering both areas (CH-CHA, 393 m a.s.l.) (Table 1).

Management practices carried out at the studied grassland sites included the application of inorganic and organic fertilizer, mowing and grazing. The amount and type of fertilizer, the frequency of cutting and the intensity and duration of grazing at the different sites were highly variable (Table 1). Thirteen of the 14 sites were fertilized between one and six times per year. Organic fertilizer was applied at 12 of the 14 sites, ranging from 33 to 365 kg N ha⁻¹ yr⁻¹. The amount of organic fertilizer spread at CH-AWS when cattle were grazing was unknown. Synthetic fertilizer was applied only at FR-LAQ-I (214 kg N ha⁻¹ yr⁻¹) and CH-CHA (2012: 17 kg N ha⁻¹ yr⁻¹), but only at CH-CHA in combination with slurry. Of the 14 sites, only one was not

fertilized during the investigated time period (FR-LAQ-E). However, for all grazed sites additional N input came from excretion of grazing animals onto the pasture.

Ten sites were cut at least once per year, whereas some intensively managed sites were cut up to five times per year. Ten sites were grazed by cattle and / or sheep between 1 - 170 days yr⁻¹. CH-CHA was ploughed for grassland restoration and resown in early 2012. Further details including key references for each site are given in Table 1.

Flux measurements

The net ecosystem exchange of the three major GHGs (CO_2 , N_2O , and CH_4) was calculated using the eddy covariance (EC, Baldocchi *et al.*, 1988) or chamber techniques, whereby for the latter either automatic (AC) or manual chambers (MC) were used (Table 1). Data availability and temporal resolution of measurements of the three targeted GHGs varied considerably across all sites. N_2O fluxes were available from all 14 sites, while CO_2 fluxes were available from ten and CH_4 fluxes from 13 sites (Figure 1). Measurement campaigns at the sites lasted between six months (AT-STU-P) and more than five years (FR-LAQ-I, FR-LAQ-E) (Table S2).

Measurements covering all three GHGs over at least one full year were available from eight sites, with results from two sites based on continuous EC measurements (AT-NEU, CH-CHA) and from six sites based on EC in combination with MC measurements (CH-AWS, CH-FRU-I, CH-FRU-E, DE-FEN-I, CH-CHA-I1, CH-CHA-I2,). CO₂ measurements for CH-AWS were only available during the growing season. Two sites had CO₂ and N₂O data available for multiple years, but no (FR-LAQ-E) or limited (FR-LAQ-I during two grazing seasons) CH₄ measurements. Measurements of N₂O and CH₄ without simultaneous CO₂ measurements were carried out at four sites, either over multiple years (DE-GAP, DE-FEN-E) or over one growing season only (AT-STU-P, AT-STU-M). Generally, data coverage was lowest for sites sampled with MCs (20 - 93 measurement days) and highest for AC and EC sites (318 - 1373 measurement days). Additional details on flux calculation methods as well as site and instrument setup are given in Table 1 and in the Supplement.

Daily average (DA) flux values were used for analyses in this study. Due to the different temporal resolutions of the measurement methods, the calculation of DA fluxes for each site and day followed different approaches: for chamber measurements, mean values across all replicates were calculated. When at least one replicate average was available for a given day (MC, AC), the flux was assumed to be representative for the whole day (24 hours). For EC data, daily average fluxes were calculated from a minimum of 21 half-hourly flux values. Applying these minimum thresholds resulted in a tradeoff between overall data availability and representativity of a given calculated daily average flux.

Flux rates in this study are given as mg CO₂ m⁻² h⁻¹ for CO₂, and μ g m⁻² h⁻¹ for N₂O and CH₄. Fluxes are reported following the convention used in micrometeorology, where positive fluxes mean a transport from the ecosystem to the atmosphere, negative fluxes mean the opposite.

Gap-filling

Fluxes were gap-filled for the calculation of site-specific GHG budgets, N₂O-N emission factors (EFs) and NGBs. While CO₂ fluxes were gap-filled following Reichstein et al. (2005), the gapfilling (GF) for N₂O and CH₄ was based on a running median (RM) approach, which comprised several steps. First, the continuous RM DA flux was calculated for each site and GHG using predefined time windows of varying lengths, selected as to best describe the measured DA flux pattern over the course of a full year. For sites where multiple years of measured N₂O data were

available, the calculation of the RM was based on the average of all available fluxes for a specific day of the year, except for CH-CHA, where the ploughing year 2012 and the following year 2013 were treated separately. Typical sizes of the RM time window were 15 - 120, 60, 60 days for MC, AC, EC data, respectively (Table 1). Potential remaining data gaps at the beginning and end of specific years were then filled by repeating the median flux value closest to the gap. This yielded a continuous estimate for the RM flux of a site for each day and year. The main reason for choosing the RM approach was that it is less sensitive to outliers, i.e. to sharp emission peaks in the data, in contrast to filling data gaps with the arithmetic mean or by linear interpolation. Second, the RM daily average flux time series was then used to substitute data gaps in the measured daily average time series with the corresponding RM value of the given day of the year, resulting in complete, gap-filled N₂O and CH₄ flux time series for the year. The RM method consequently leads to cumulative fluxes representative for a given site, but it is not suitable for predicting or simulating GHG emission pulses, e.g. as a consequence of management or freeze/thaw periods. Thus, budgets calculated from the RM method are likely to underestimate the "true" budget at a specific site. From the grazed meadow FR-LAQ-I, CH₄ measurements were only available during the growing season with cattle present in the measurement footprint. To achieve year-round CH₄ budgets, time periods without cattle were gap-filled with a constant, low CH₄ emission value (160 μ g m⁻² h⁻¹), similar to flux rates observed during ungrazed time periods at another site in an earlier study (Dumortier et al., 2017).

Ancillary data

Measurements of ancillary data included ambient air temperature (TA in °C), soil temperature (TS in °C), soil water content (SWC in vol. %), and precipitation (mm) (Table 1). Measured soil

parameters were bulk density (BD) and pH. SWC was converted to water-filled pore space (WFPS) by first calculating the total porosity (TP) of the soil in percent for each site as

$$TP = \left(1 - \frac{BD}{PD}\right) \qquad , \tag{2}$$

where BD is the bulk density for each site and PD is the particle density assumed as 2.65 g cm⁻³. In a second step, TP (%) was used to calculate WFPS (%) following

$$WFPS = \left(\frac{SWC}{TP}\right),\tag{3}$$

where SWC is the soil water content (volumetric %) as measured at each site.

Normalization

In order to identify environmental conditions conducive to enhanced GHG source/sink activity, measured non-gapfilled daily average N₂O and CH₄ fluxes were investigated in relation to different combined classes of the two potential drivers soil temperature (TS) and soil moisture (given in water-filled pore space, WFPS). One approach to account for diverse environmental conditions and soil physical properties while also improving comparability across sites is the normalization of all involved variables to their respective percentile values at site level. Daily average flux values of N₂O and CH₄ fluxes, as well as TS and WFPS measurements at each site were converted to an index in the range 0 to 100% based on the cumulative empirical probability density function (cePDF) of each variable at each site. That is, the index value corresponds with the percentile value of the original measurements in relation to the site-specific cePDF. These index values were further aggregated in graphical displays by showing the median of the index values from all sites within each aggregation unit. Following this approach facilitated the identification of common emission/deposition sweet spots, i.e. environmental conditions that

contribute to an increase or decrease of GHG fluxes. The use of strictly linear, site-specific percentile values for sweet spot analyses had the advantage of investigating fluxes in relation to site-specific ranges of potential drivers (Luo *et al.*, 2013).

For the quantification of the fertilization effect, daily average fluxes in the period starting 7 days before and ending 7 days after the event were normalized by the 7-day flux average before the event, not including the day of the event (day 0) (see Figure 8 and 9).

Data analysis

Site-specific of N₂O-N emission factors (EFs) are expressed as the ratio between annual N₂O-N budgets after gap-filling and the amount of applied fertilizer. Results from multiple linear regression analyses (MLR) were checked for multicollinearity by inspecting the eigenvalues of soil temperature and water-filled pore space in a correlation matrix. Eigenvalues across all sites were found between 0.37 and 1.63, indicating no multicollinearity problems. The adjusted coefficient of determination (r_{adj}^2) corresponds to r^2 after adjustment based on the degrees of freedom of the respective model, i.e. r^2 is adjusted to the number of regressors and the sample size. As such, r_{adj}^2 is an indicator for the utility of a regression model, especially for MLR models, by describing the explained variation in the dependent variable above what would be expected by chance. Data analyses were based on daily average values. Plots and statistical analyses were done using the free and open source programming language *Python* (version 3.6.0, Python Software Foundation), including the packages pandas (version 0.20.3; McKinney, 2010), numpy (version 1.13.1; Van Der Walt et al., 2011), matplotlib (version 2.0.2; Hunter, 2007) and statsmodels (version 0.8.0; Seabold & Perktold, 2010). Significance levels given in regression analyses correspond to the two-tailed P-values using Wald Test with t-distribution of the test

statistic. Sites included in figures and tables of this manuscript are listed in descending order of elevation from top to bottom and left to right. Average values are given \pm standard error of the mean (SEM) where possible.

Results

Greenhouse gas measurements

The CO₂ flux was available from nine sites and showed highest net CO₂ uptake during spring and summer, reflecting time periods of high plant productivity (Figure 2a). During these warmer seasons, measured median fluxes ranged between -1.02 (AT-NEU in spring) and -0.09 mg CO₂ m⁻² h⁻¹ (CH-FRU-E in spring), except for spring at CH-CHA, which was characterized by net CO₂ losses (0.12 mg CO₂ m⁻² h⁻¹). Measured CO₂ uptake generally decreased during colder months, with measurements indicating small uptake or emission of CO₂ (-0.28 to 0.28 mg CO₂ m⁻² h⁻¹). The average annual CO₂ flux across all sites, calculated from gap-filled data, was -1426 ± 248 g CO₂ m⁻² yr⁻¹, with strongest CO₂ uptake in spring (-855 ± 80 g CO₂ m⁻²), followed by summer (-577 ± 100 g CO₂ m⁻²) and autumn (-131 ± 83 g CO₂ m⁻²). Winter was on average a CO₂ source (137 ± 52 g CO₂ m⁻²).

 N_2O was emitted from all grasslands and during all seasons, except for AT-NEU, where small uptake rates of -2 µg N_2O m⁻² h⁻¹ were recorded during spring (Figure 2b). The median of directly measured seasonal fluxes at the emitting sites ranged between 0.1 (FR-LAQ-I in winter) and 240 µg N_2O m⁻² h⁻¹ (CH-CHA-I2 in summer). The average annual N_2O flux across all sites, calculated from gap-filled data was 2664 ± 1024 mg N_2O m⁻² yr⁻¹, with strongest emissions in summer (1063 ± 381 mg N_2O m⁻²) and weakest emissions during winter (422 ± 204 mg N_2O m⁻²).

Median seasonal CH₄ fluxes calculated from chamber measurements were generally negative, ranging between -46 (AT-STU-M) and -6 μ g CH₄ m⁻² h⁻¹ (DE-FEN-I), indicating uptake of atmospheric CH₄ by grassland soils (Figure 2c). Methane chamber emissions were found only during winter at four sites (CH-FRU-I, DE-GAP, CH-CHA-I1, CH-CHA-I2; ranging between 0.3 and 8 μ g CH₄ m⁻² h⁻¹). In contrast to chamber measurements, median CH₄ fluxes from EC measurements were all positive during all seasons, with highest emissions observed at FR-LAQ-I during spring when cattle were present within the flux footprint (4565 μ g CH₄ m⁻² h⁻¹). After gap-filling, the average CH₄ flux across all sites, not including FR-LAQ-I, amounted to 36 ± 85 mg CH₄ m⁻² yr⁻¹, with strongest CH₄ emissions in autumn (18 ± 22 mg CH₄ m⁻²).

Effect of two drivers on N₂O and CH₄ exchange

The identification of GHG source/sink sweet spots in relation to specific soil moisture and temperature conditions at the site level worked best with sites where flux measurements were taken at high temporal resolution, i.e. based on EC and AC measurements (Figure 3, Figure 4). For example, N₂O emissions at FR-LAQ-I were highest when WFPS was above 75% and lowest with TS below 5°C, conditions during which low emissions could also translate into small uptake of N₂O (Figure 3a, Table 2). However, other sites deviated from this observation. N₂O emissions at AT-NEU were highest with TS above 15°C or below 5°C and WFPS around or below 50%. Similar emission patterns were also found at DE-FEN-E, with highest emissions occurring at TS > 15°C or < 5°C, and lowest N₂O emissions with WFPS < 50%. CH-CHA was the only site where WFPS frequently exceeded 90% (interquartile range: 85 – 94%). During these overall wet conditions, when the soil was almost fully water-saturated, observed N₂O emissions at CH-CHA were low. Chamber measurements at the same site in previous years, prior to grassland restoration, revealed a somewhat contrasting flux pattern, but were performed during generally

warmer time periods (data not shown). Merging all site-level observations showed that the highest N₂O percentile flux generally occurred during warm and wet periods, with considerably lower percentile fluxes during colder time periods (Figure 3b).

In comparison to N₂O, the investigation of CH₄ at site level revealed flux patterns that in many cases were dominated by uptake of atmospheric CH₄ by soils (Figure 4a). Therefore, interpreting flux patterns was more challenging because most sites could act both as a clear sink or a source for CH₄ during different time periods. Thus, upper flux percentiles did not necessarily reflect CH₄ emission, but equated to low CH₄ uptake at some sites. Across 13 investigated sites for which CH₄ measurements were available, ten sites were dominated by CH₄ uptake, with only two sites (AT-NEU, CH-CHA) showing clear emission patterns, not including FR-LAQ-I (Table 2, Figure 4a). Both DE-FEN-I and DE-FEN-E showed highest CH₄ uptake with TS > 15°C and WFPS < 50%, weakest CH₄ uptake was observed with WFPS above or around 50% (DE-FEN-I, DE-FEN-E) and TS < 10°C (DE-FEN-E). For AT-NEU, uptake was mainly observed at intermediate WFPS and TS around 10°C, while highest CH₄ emissions occurred with TS > 10°C (Figure 4a). Across all sites, the CH₄ percentile flux increased with increasing WFPS and decreasing TS (Figure 4b).

Normalized N₂O and CH₄ flux patterns across all sites, based on the same classes of TS and WFPS as shown in Figure 3b and Figure 4b could well be explained by either TS or WFPS in a simple linear regression (Figure 5). Soil temperature was a significant driver for N₂O ($r^2 = 0.88$, *P* < 0.001) and CH₄ fluxes ($r^2=0.35$, *P* < 0.05). WFPS had high predictive power for CH₄ exchange ($r^2 = 0.84$, *P* < 0.001) and was a significant driver for N₂O fluxes ($r^2 = 0.54$, *P* < 0.05).

In order to test if the predictive power of TS and WFPS for flux percentiles across all sites also succeeds at the site level, multiple linear regression (MLR) and simple linear regression (SLR)

analyses were performed on measured, log-transformed daily average N₂O and CH₄ fluxes for each site. Data included in these analyses were not gap-filled, measured during snow-free conditions and not directly disturbed by cutting and fertilization management events, i.e. data from the three days directly after a management event were excluded from these analyses (Table 3). The explained variance of N₂O fluxes in a MLR was low for most sites, with a coefficient of determination (r^2) of 0.19 on average, ranging between 0.02 (DE-FEN-E) and 0.47 (CH-FRU-E). TS as predictor variable in a SLR at site level generally explained only a small fraction of observed flux patterns (significant r^2 between 0.01 and 0.27), similarly low values were found for WFPS (significant r^2 between 0.01 and 0.29).

Similar to N₂O fluxes, the combined explanatory power of the potential driver variables TS and WFPS for observed CH₄ flux patterns was limited ($r^2 = 0.23$, on average), but yielded good results for the extensive high altitude site CH-AWS ($r^2 = 0.77$). For the remaining sites, significant r^2 ranged between 0.04 (AT-NEU) and 0.40 (CH-FRU-E, DE-GAP). The explained variance for subdivided sites was higher for the less intensively managed part of the grassland. For example, r^2 was higher for CH-FRU-E than for CH-FRU-I ($r^2 = 0.40$ vs. 0.19), and higher for DE-FEN-E than for DE-FEN-I ($r^2 = 0.32$ vs. 0.22). The SLR identified WFPS as a relatively good predictor variable for the high altitude site CH-AWS ($r^2 = 0.72$). However, the high predictive power of TS and WFPS for percentile-normalized N₂O and CH₄ fluxes, respectively, across all sites (Figure 5) was not supported by MLR and SLR analyses of log-transformed data at site level.

Regression analyses indicated that the role of the two potential driver variables TS and WFPS in driving N_2O and CH_4 fluxes can be vastly different across sites, i.e. the spatial domain (Table 3). Therefore, in a next step, we analyzed their predictive power for measured, non-gapfilled data in

the temporal domain. To this end, we investigated the explained variance of observed N₂O and CH₄ fluxes by the combined use of TS and WFPS as predictors in a moving 35-day time window (Figure 6, Figure 7). In order to perform this analysis, long-term data recorded at high temporal resolution were required. This requirement was met by six sites in this study, namely those that used either EC or AC measurements for the quantification of N₂O or CH₄ fluxes (FR-LAQ-I, FR-LAQ-E, AT-NEU, DE-FEN-I, DE-FEN-E, CH-CHA). The analysis revealed that the role of WFPS and TS as driving variables of observed fluxes varied considerably over the course of the measurement periods. During the growing season, both variables often predicted observed N_2O fluxes with high precision and significance (P < 0.05), with maximum r² ranging between 0.71 (AT-NEU in summer 2010) and 0.90 (DE-FEN-E in summer 2012) for individual sites (Figure 6). In contrast, their explanatory value was low and often close to zero during cold time periods and snow cover when N₂O fluxes were low. Especially for N₂O fluxes, results during certain time windows were often in strong contrast to results from the MLR analyses in Table 3. For example, at DE-FEN-E, WFPS and TS were poorly correlated with N₂O fluxes with all measurements considered ($r^2 = 0.02$, Table 3), but both predictors explained up to 90% of observed fluxes between 25 June and 30 July 2012 at the same site (Figure 6). Similar results were also found for CH₄, with maximum r^2 between 0.41 (AT-NEU autumn/winter 2010) and 0.92 (DE-FEN-I and DE-FEN-E in summer/autumn 2013) in certain time windows (Figure 7). Generally, using TS and WFPS as predictors for measured fluxes in pre-defined time windows yielded better and more significant results for N_2O than for CH_4 (Figure 6, Figure 7).

Fertilization effect on N₂O and CH₄ fluxes

The availability of flux measurements for the time period before, during and after fertilization events allowed for an evaluation of the management impact on observed N_2O and CH_4 exchange.

Flux data around multiple fertilization dates were available from three grasslands, all of which used slurry as fertilizer (DE-FEN-I, DE-FEN-E, CH-CHA). Slurry application resulted in clear N₂O emission peaks at all three sites either on the day of application or during the following 7 days (Figure 8). In comparison to the seven days preceding the application, N₂O emissions across all sites were on average 10 times higher on the day of fertilization, 5 times higher one day after fertilization, and 2 times higher over the following six days. N₂O fluxes stayed elevated for a few days after the event, reaching pre-fertilization flux rates again on day 3 – 7 after fertilizer application. Average N₂O emission rates during the seven days before management for CH-CHA (125 ± 45 μ g N₂O m⁻² h⁻¹ on average) were high in comparison to DE-FEN-I (23 ± 7 μ g N₂O m⁻² h⁻¹).

The high N₂O emissions after fertilization of the grassland had a strong impact on the total amount of N₂O-N that was emitted from the respective grassland to the atmosphere over the course of the year. For example, cumulative N₂O-N emissions from the grassland at CH-CHA amounted to 2.6 kg N ha⁻¹ over the course of 2013 (Table 6). During the same year, 0.7 kg N ha⁻¹ were emitted immediately after four fertilization events, i.e. N₂O-N emissions over the course of the fertilization day and the following week after subtraction of pre-fertilization flux rates, which is equal to 28% of the annual cumulative N₂O-N emissions. Hence, each fertilizer application resulted in immediate N₂O-N emissions of 7 ± 1% of the annual cumulative loss. Similar results were also found at DE-FEN-I between 2012 and 2014 (7 ± 2% per fertilization), demonstrating the impact of fertilizer application on the annual N₂O budget.

Similar to N_2O emissions, CH_4 fluxes were elevated on the day of slurry application (Figure 9). However, methane emissions decreased earlier in comparison to N_2O emissions and reached prefertilization values one or two days after fertilization. Unlike N_2O , the grasslands at DE-FEN-I

and DE-FEN-E were a CH₄ sink before fertilizer application, albeit flux averages were characterized by high standard errors. For DE-FEN-I and DE-FEN-E, average CH₄ uptake rates of -11 \pm 3 and -26 \pm 19 µg m⁻² h⁻¹, respectively, were found over the course of the seven days preceding management. Manure application turned the two grasslands from a sink to a source of CH₄, with high emissions on the day of fertilization (1271 \pm 440 and 212 \pm 250 µg m⁻² h⁻¹, respectively) and a rapid decrease of CH₄ emissions in the following week (-4 \pm 8 and -25 \pm 16 µg m⁻² h⁻¹, respectively). In contrast, the grassland at CH-CHA was mostly a CH₄ source before fertilization (17 \pm 78 µg m⁻² h⁻¹), with elevated emission peaks on the day of slurry application (637 \pm 239 µg m⁻² h⁻¹) and CH₄ emission rates that stayed elevated during the week after fertilization (228 \pm 72 µg m⁻² h⁻¹).

GHG budgets

In-situ measurements over multiple years in combination with subsequent gap-filling allowed for the calculation of site-specific annual GHG budgets (Table 4). During the investigated time periods in this study, all ten sites for which the CO₂ flux was quantified for at least one year were a CO₂ sink, ranging between -2806 g CO₂ m⁻² yr⁻¹ (CH-FRU-I) and -91 \pm 20 g CO₂ m⁻² yr⁻¹ (AT-NEU, 2010-2011). All 14 sites with N₂O measurements were a N₂O source, emitting between 18 g CO₂ m⁻² yr⁻¹ (AT-STU-P) and 638 \pm 519 g CO₂ m⁻² yr⁻¹ (CH-CHA, 2012-2013). Findings for the 13 sites with CH₄ measurements were more diverse, with nine sites acting as a methane sink, ranging between -9 g CO₂-eq. m⁻² yr⁻¹ (CH-AWS, AT-STU-M) and -1 \pm 2 g CO₂-eq. m⁻² yr⁻¹ (DE-GAP, 2012-2013; DE-FEN-I, 2012-2014). Three sites (AT-NEU, DE-FEN-I, CH-CHA) were a CH₄ source (3 to 41 CO₂-eq. m⁻² yr⁻¹). Strongest CH₄ emissions were found for the heavily grazed FR-LAQ-I, where cattle were present in the EC footprint, amounting to 488 \pm 100 CO₂eq. m⁻² yr⁻¹ on average between 2010 and 2011 (Table 4).

The full NGB was calculated for nine sites where concurrent measurements of all three GHGs (CO₂, N₂O, CH₄) were available. Despite the offset of CO₂ uptake by mainly N₂O and to some extent CH₄ emissions, the NGB of the grasslands was strongly negative, with minimum and maximum CO₂-eq. uptake of -58 ± 32 g CO₂-eq. m⁻² yr⁻¹ (AT-NEU, 2010-2011) and -2761 g CO₂-eq. m⁻² yr⁻¹ (CH-FRU-I), respectively (Table 4). The annual CO₂ sink strength of the grasslands was offset by concurrent N₂O and CH₄ fluxes by between 2% (CH-FRU-I) and 48% (FR-LAQ-I, 2008-2013). On average across all sites, the CO₂ flux offset amounted to 21 ± 6% (Table 4).

The fluxes of all three GHGs (CO₂, N₂O and CH₄) were generally characterized by strong interannual variability (Table 4). For example, CO₂ uptake at FR-LAQ-I between 2008 and 2011 was found between -1537 and -814 g CO₂ m⁻² yr⁻¹. During the same time period, N₂O emissions (between 48 and 247 g CO₂-eq. m⁻² yr⁻¹) offset the CO₂ uptake by 6 – 17%. The biggest difference between years was found for CH-CHA, where grassland restoration in 2012 included ploughing, sowing, fertilizer and pesticide application as well as regular harvests. In the same year, the first resowing after ploughing failed and vegetation was almost absent until summer. The NGB of CH-CHA during the restoration year 2012 amounted to 2446 g CO₂-eq. m⁻²-the highest across all sites-as a consequence of high CO₂ (1246 g CO₂ m⁻²) and N₂O emissions (1157 g CO₂-eq. m⁻²), along with relatively low CH₄ emissions (43 g CO₂-eq. m⁻²; Table 4). However, in 2013, CH-CHA changed from being a GHG source to a strong GHG sink (-4514 g CO₂-eq. m⁻²), with high CO₂ uptake (-4671 g CO₂ m⁻²) and considerably lower N₂O emissions (119 g CO₂eq. m⁻²), while CH₄ emissions remained similar (38 g CO₂-eq. m⁻²). The inter-annual variability of CH₄ fluxes was generally lower than that of CO₂ and N₂O fluxes (Table 4).

Historically, considerably more measurements are available for grassland CO₂ fluxes, while data for N₂O and CH₄ remain still relatively sparse. Therefore, we set site-specific budgets presented in this study in relation to previous studies that investigated N₂O and CH₄ exchange over grasslands (Table 5). Out of 46 sites with N_2O measurements (including sites in this study), 43 sites were on average N_2O sources, albeit over sometimes vastly different measurement campaign lengths (Table 5). In the literature, we found N₂O fluxes from 13 European grasslands where measurements covered at least one full year and management was similar to sites investigated in this study (grasslands with ID 23, 24, 32, 34, 38-40, 44, 45, 49-52 in Table 5). At these sites, the overall yearly flux average amounted to $43 \pm 21 \ \mu g \ N_2 O \ m^{-2} \ h^{-1}$, similar to average fluxes of $55 \pm 10^{-2} \ h^{-1}$ 21 μ g N₂O m⁻² h⁻¹ from the twelve sites with year-round measurements in this study (Table 5). The comparison of CH₄ fluxes across sites is more challenging, as some sites reported CH₄ flux rates with or without considering grazing animals in the investigated area (Table 5). We found that CH₄ flux rates from EC measurements for the grazed site FR-LAQ-I (yearly average: $1639 \pm$ 336 μ g CH₄ m⁻² h⁻¹) were comparable to sites that used the SF₆ tracer technique (ID 52: 1021 μ g CH₄ m⁻² h⁻¹, ID 44: 1288 μ g CH₄ m⁻² h⁻¹; Soussana *et al.*, 2007b) and to a recent EC study at a Belgian pasture with cattle in the flux footprint (ID 30: 1107 μ g CH₄ m⁻² h⁻¹; Dumortier *et al.*, 2017b). Methane emissions found for FR-LAQ-I were also in the same order of magnitude as emissions from a fen meadow (ID 40, Kroon et al., 2010) and a peatland pasture (ID 29, Baldocchi et al., 2012), but much lower than emissions from a flooded grassland (ID 20, Hernandez *et al.*, 2014). Excluding peatlands, CH_4 fluxes were generally low and found between -59 and 136 μ g CH₄ m⁻² h⁻¹, when cattle were not considered in flux calculations. In total, 17 of 41 sites with CH₄ measurements, including sites in this study, reported uptake over yearly or shorter time horizons (Table 5).

The availability of gap-filled N₂O measurements for all ten fertilized sites in combination with detailed information about the amount of fertilizer applied to the grassland enabled the calculation of yearly N₂O-N emission factors (EFs; Table 6). After gap-filling, N₂O budgets for a total of 21 years were available. Minimum cumulative N₂O-N emissions as well as the lowest EF were found for AT-NEU in 2010 (0.19 kg N ha⁻¹; EF: 0.1%), while maximum emissions and the highest EF were found for CH-CHA during the restauration year in 2012 (24.70 kg N ha⁻¹; EF: 8.6%). For the sites where several years of data were available, cumulative N₂O-N emissions and EFs were found to vary between years. For example, emissions ranged from 0.57 to 5.28 kg N ha⁻¹ yr⁻¹ at FR-LAQ-I between 2008 and 2013, corresponding to EFs of 0.3 – 2.5%. Our findings indicate that the ten fertilized sites in this study emitted on average $1.8 \pm 0.5\%$ of the applied fertilizer N back to the atmosphere (Table 6).

Discussion

Soil environmental conditions can influence N_2O and CH_4 fluxes by providing ideal conditions for GHG producing or consuming microbial communities (Li *et al.*, 1992; Holtan-Hartwig *et al.*, 2002; Barnard *et al.*, 2005; Dijkstra *et al.*, 2013). Therefore, we expected clear relationships between soil conditions and magnitude of fluxes across timescales. However, regression analyses for site-level flux observations revealed low or inconsistent explanatory power of TS and WFPS (Table 3, Figure 6, Figure 7). The role of the two variables as flux drivers became more apparent after identification of site-specific GHG sweet spots (Figure 3, Figure 4). Low N₂O emissions at CH-CHA during wet conditions could be the consequence of increased N₂O reduction to N₂ during denitrification compared to production (Figure 3a). When the soil water content is high, the available time for the reduction of N₂O to N₂ during the last step of denitrification is increased, reducing N₂O release to the atmosphere (Clough *et al.*, 2005; Wu *et al.*, 2013). The

clear N₂O uptake in intermediate TS classes at AT-NEU indicated time periods when N₂O reduction in the soil exceeded concurrent N₂O production (Figure 3a; Chapuis-Lardy *et al.*, 2007; Hörtnagl & Wohlfahrt, 2014). However, based on available data it was not possible to conclude whether the observed net uptake was the consequence of increased reduction of N₂O, e.g. due to increased respiration of heterotrophic bacteria, or reduced N₂O production rates, e.g. due to cool temperatures (Chapuis-Lardy *et al.*, 2007). Still, at AT-NEU, the observation of clear N₂O uptake with TS < 10°C and WFPS < 50% but clear N₂O emission at TS > 10°C during similar soil moisture conditions suggests that reduced N₂O production rates were the main driver behind measured net N₂O uptake in this soil moisture range. At the same time, N₂O uptake at relatively high WFPS > 50% could be mainly the consequence of increased reduction rates (Figure 3a; Wu *et al.*, 2013).

Generally, the warming effect on N₂O fluxes was inconsistent at site level, similar to findings from other studies (e.g., Bijoor *et al.*, 2008; Hu *et al.*, 2010). Across all sites, the clear relationship between N₂O fluxes and TS indicated that increasing temperature fuels denitrification turnover processes in the soil, leading to enhanced N₂O emissions (Figure 3b, Figure 5a). Elevated N₂O fluxes at low TS were probably the consequence of emission bursts during freeze/thaw cycles (Risk *et al.*, 2013). For CH₄, reduced percentile fluxes at high TS in combination with relatively low WFPS both across all grassland sites (Figure 5b) and at the sitelevel (e.g. DE-FEN-E, Figure 4) are in contrast to findings for wetlands, rice paddies and aquatic ecosystems (Yvon-Durocher *et al.*, 2014), but similar to findings for montane grasslands (Unteregelsbacher *et al.*, 2013). The strong correlation between CH₄ fluxes and WFPS is supported by previous studies (Le Mer & Roger, 2001; Wang *et al.*, 2015; Hofmann *et al.*, 2016).

Site-specific properties of managed grasslands have the potential to change over relatively short timescales, depending on the frequency and intensity of management events along with environmental conditions. For example, trampling by grazing animals or use of heavy machinery can increase soil compaction and negatively impact soil structure (Ball, 2013). This in turn can affect soil conditions crucial to the production or consumption of GHGs in the soil, such as WFPS. Furthermore, the input of external fertilizer affects nutrient availability in the soil to varying extends and can also impact soil pH, depending on fertilizer type and amount as well as the timing of its application (Saggar et al., 2013). Thus, GHG emissions/deposition sweet spots are not only different among sites (Figure 3, Figure 4), but are also most likely not persistent, depending on applied management strategies, environmental conditions and shifting microbial communities in response thereof (Jones et al., 2014). The detection of sweet spots is therefore of high interest for developing site-specific GHG mitigation strategies, which need to be adapted over the course of a year. For example, the knowledge about sweet spots could assist in scheduling site-specific fertilization dates in such a way that fertilizer is only applied during time periods with low GHG emission impact, i.e. when the normalized flux in specific combined classes of the two potential drivers TS and WFPS is known to be low (Figure 3, Figure 4). In addition, significant relationships between normalized fluxes and potential drivers across sites indicated that site-specific data normalization prior to analyses could facilitate the detection of correlations (Figure 5) and thus improve methods for calculating GHG budgets on a continental scale.

The application of slurry coincided with elevated N_2O emissions (Figure 8), which is in accordance with findings in earlier studies (Neftel *et al.*, 2010; Jones *et al.*, 2011). Increased N_2O emissions were expected, as N input via fertilization constitutes the most concentrated input of

anthropogenic N, with high soil N availability fueling N_2O production by nitrifying/denitrifying bacterial communities (Firestone & Davidson, 1989; Davidson, 2009). The high impact of fertilization on N2O emissions at CH-CHA were probably the consequence of generally warm temperatures around 20°C in combination with considerably wetter soil conditions in comparison to DE-FEN-I and DE-FEN-E. After some fertilization applications, N₂O emissions stayed elevated the longest with warm or increasing TS in combination with WFPS quickly decreasing from high to intermediate values, for example on 16 August 2012 at CH-CHA (Figure 8). This observation at CH-CHA could indicate that N₂O emissions after fertilizer application were additionally fueled due to decreasing reduction rates of N2O to N2 as a consequence of declining WFPS (Wu et al., 2013). However, the exact causes why N₂O emissions stayed elevated over a given period of time are difficult to determine without additional measurements, such as soil oxygen and substrate availability. For CH-CHA during the restoration year 2012, soil water content, soil and air temperature, N input via fertilization and the net CO_2 exchange as a proxy for plant activity were identified as potential drivers for measured N₂O fluxes (Merbold et al., 2014). The same study found reduced N_2O -N EFs during time periods of high productivity or vice versa, suggesting a fast turnover of mineral N as possible explanation for this observation. However, in this study we were not able to replicate this finding at the annual timescale, as the relationship between net CO₂ flux and N₂O-N EFs across sites was generally low (data not shown). With the average N₂O-N EF across sites in this study being clearly higher than the IPCC Tier 1 EF of 1% and given the high variability of N₂O-N EFs across site-years, more direct long-term measurements are needed to improve and develop sophisticated Tier 2 and Tier 3 EFs for their application at the national scale (IPCC, 2006; Table 6).

Emission peaks after slurry application were also observed for CH₄ and supported earlier findings (e.g. Mori & Hojito, 2015). However, at DE-FEN-I and DE-FEN-E, CH₄ emissions decreased more rapidly to pre-fertilization levels than N₂O fluxes, suggesting that large amounts of CH₄ were released from the slurry itself as opposed to being produced in the soil (Chadwick *et al.*, 2000). In contrast, elevated CH₄ emissions at CH-CHA after fertilization suggested that small amounts of CH₄ were produced in the soil, possibly from organic matter supplied in the slurry, i.e. through the microbial degradation of volatile fatty acids (Sherlock et al., 2002). Furthermore, CH₄ oxidation by soil microorganisms was possibly reduced due to elevated NH₄⁺ soil concentrations following N fertilizer applications inhibiting the CH₄ oxidation capacity, effectively increasing emissions from the soil (Bodelier & Laanbroek, 2004). The different emission patterns at CH-CHA and DE-FEN-I/DE-FEN-E after fertilizer application are probably due to the respective measurement methods at the sites (Figure 8). Eddy covariance fluxes at CH-CHA are based on an integral signal calculated from high-frequency samples from the whole footprint, comprising both hot spots of high CH₄ emissions but also smaller areas of CH₄ uptake (Baldocchi et al., 2012). In comparison, chamber measurements at DE-FEN-I and DE-FEN-E represent the exchange over a much smaller area of the grassland, resulting in a more immediate response of the measured signal to fertilizer application in the chambers. Due to this small-scale variability being an integral component of the EC method, fluxes are probably dampened and lower than what would be expected from laboratory or chamber experiments.

At all sites presented in this manuscript, the CO_2 flux was the predominant component of the annual GHG budget (Table 4). Our observation that N₂O and CH₄ emissions in terms of CO₂-equivalents offset 21 ± 6% of concurrent CO₂ uptake is similar to the 18% reported for European grasslands (Schulze et al., 2009). Even at the heavily grazed site FR-LAQ-I, which was

characterized by high ruminant CH_4 emissions by grazing animals in the EC flux footprint, the grassland was a clear GHG sink (Table 4), supporting earlier observations (Chang et al., 2015). Still, high CH_4 emissions at FR-LAQ-I highlighted the need to consider grazing cattle during the evaluation of grassland GHG budgets (e.g., Martin *et al.*, 2010).

We found that year-round GHG measurements are necessary for unbiased GHG budget calculations, mainly due to relevant N₂O and CH₄ flux contributions during spring and winter (Figure 2). Spring N₂O emissions were most likely dominated either by freeze-thaw emission bursts or high soil moisture conditions after snowmelt (Risk *et al.*, 2013), winter N₂O production can still occur at low temperatures in frozen soil (Teepe *et al.*, 2001; Zhu *et al.*, 2005; Wertz *et al.*, 2013). For CH₄, we assume that seasonal fluxes were mainly driven by the presence or absence of anaerobic CH₄-producing microsites in the soil, the application of slurry as fertilizer, as well as temperature (Chadwick *et al.*, 2000; Treat *et al.*, 2014). The role of snow accumulation during winter on observed CH₄ emissions needs further investigation (Blanc-Betes *et al.*, 2016).

Direct long-term measurements at site level are of highest importance to quantify the annual GHG exchange. With N₂O and CH₄ flux gap-filling being a source of uncertainty, continuous GHG measurements at high temporal resolution are crucial for reliable GHG budget estimates (Mishurov & Kiely, 2011; Barton *et al.*, 2015). In this study, the availability of high-resolution data from AC and EC measurements facilitated the application of advanced statistical methods, e.g. the quantification of fertilization impacts on GHG fluxes (Figure 8, Figure 9). For future studies, we recommend simultaneous chamber and EC measurements in the same flux footprint to investigate potential biases of the different methods (Eugster & Merbold, 2015). Reducing the uncertainty in quantifying N₂O and CH₄ budgets at the site level is ideally done using a multi-step approach and comprises (1) spatial snapshot measurements of small areas for the identification of

emission hot spots in order to understand footprint source/sink heterogeneity, (2) capturing temporal high fluxes, and (3) identifying environmental conditions that indicate enhanced GHG source/sink activity, i.e. sweet spots. While (1) is best achieved via chamber measurements using multiple plots (Skiba et al., 2009; Cowan et al., 2015), (2) and (3) are best investigated via longterm automatic chamber or eddy covariance measurements at high temporal resolution, thus covering a wide range of environmental conditions while considering spatial information from (1) during data interpretation. For grazed sites, knowledge of animal movements and distribution of manure pats in the flux footprint have to be considered for in depth analyses of GHG source/sink behavior (Felber et al., 2015). This is of special importance for the EC method, by which smallscale emission and deposition hot spots are integrated spatially (Baldocchi et al., 2012). In addition, future research should also focus on the development and improvement of meaningful land use indices that consider specific management strategies at the site-level and aggregate available site information into objective categories. While we are aware of existing indices for land use intensity (e.g., Blüthgen et al., 2012), we refrained from applying them due to various simplifications that lead to indices lacking representativity for sites included in this study. The availability of representative, objective land use indices would allow accurate classifications of managed grasslands into meaningful categories, and thus improved statistical analyses of *in-situ* data across sites. Generally, it is challenging to attribute annual budgets to specific management strategies. The main reason for this is the finding that site-specific GHG fluxes vary considerably between years despite similar management (Table 4). This observation mandates the inclusion of extended datasets in GHG analyses that comprise comprehensive soil and management information, but also the application of advanced statistical methods (e.g., Dengel *et al.*, 2013).

Central European grassland sites in this study were characterized by site-specific management strategies that reflected the wide range of site characteristics and exemplified the complexity of managed grassland ecosystems in geographical proximity. The CO₂ sink strength as the predominant component of the annual GHG budget highlighted the need to conduct CO₂ flux measurements at the site-level. However, the impact of N₂O and CH₄ on the annual NGB of the grassland is substantial at many sites. Therefore, due to the absence of robust relationships between N₂O and CH₄ fluxes and environmental drivers, long-term *in-situ* measurements are crucial in reliably assessing the full annual NGB of specific grasslands. This is especially important during extreme management events such as grassland restoration that includes ploughing, which have the potential to change an otherwise strong annual GHG sink to a source.

Acknowledgements

We greatly acknowledge funding received from the following sources. The Swiss sites were funded by the European Union Seventh Framework Programme (FP7, 2007–2013) under grant agreement no. 244122 (GHG-Europe), the Swiss National Science Foundation under grants FasMeF (200021_129866) and FACCE-JPI project Models4Pastures (40FA40_154245) as well as the COST Action ES0804 – ABBA. This study was financially supported by the Austrian National Science Fund (FWF) under contract P23267-B16, the Tyrolean Science Fund under contract Uni-404/1083, the EU framework 7 project GHG Europe (EU contract no. 244122) and the Austrian Federal Ministry of Science, Research and Economy through an infrastructure grant. Infrastructure and work at the German sites were funded by the Helmholtz Association (01LL0801B) and the Federal Ministry of Education and Research (BMBF) via the BonaRes project SUSALPS (031B0027A). In addition, we are grateful for the help of all Grassland Sciences group members at ETH Zurich who participated in the intensive observation campaigns

at CH-CHA, CH-FRU and CH-AWS in 2010 and 2011, as well as the technical team based in Zurich, Thomas Baur, Philip Meier and Peter Plüss.

References

- Allard V, Soussana J-FF, Falcimagne R et al. (2007) The role of grazing management for the net biome productivity and greenhouse gas budget (CO₂, N₂O and CH₄) of semi-natural grassland. *Agriculture, Ecosystems & Environment*, **121**, 47–58.
- Bahn M, Rodeghiero M, Anderson-Dunn M et al. (2008) Soil respiration in European grasslands in relation to climate and assimilate supply. *Ecosystems*, **11**, 1352–1367.
- Baldocchi DD, Hincks BB, Meyers TP (1988) Measuring biosphere-atmosphere exchanges of biologically related gases with micrometeorological methods. *Ecology*, **69**, 1331–1340.
- Baldocchi D, Detto M, Sonnentag O, Verfaillie J, Teh YA, Silver W, Kelly NM (2012) The challenges of measuring methane fluxes and concentrations over a peatland pasture. *Agricultural and Forest Meteorology*, **153**, 177–187.
- Ball BC (2013) Soil structure and greenhouse gas emissions: a synthesis of 20 years of experimentation. *European Journal of Soil Science*, **64**, 357–373.
- Barnard R, Leadley PW, Hungate BA (2005) Global change, nitrification, and denitrification: A review. *Global Biogeochemical Cycles*, **19**, 1–13.
- Barnosky AD (2008) Colloquium paper: Megafauna biomass tradeoff as a driver of Quaternary and future extinctions. *Proceedings of the National Academy of Sciences of the United States of America*, **105 Suppl**, 11543–11548.
- Barton L, Wolf B, Rowlings D et al. (2015) Sampling frequency affects estimates of annual nitrous oxide fluxes. *Scientific Reports*, **5**, 15912.

- Beyer C, Liebersbach H, Höper H (2015) Multiyear greenhouse gas flux measurements on a temperate fen soil used for cropland or grassland. *Journal of Plant Nutrition and Soil Science*, **178**, 99–111.
 Bhandral R, Bolan N. SNS, Saggar S (2010) Nitrous oxide emission from farm dairy effluent application in grazed grassland. *Revista de la ciencia del suelo y nutrición vegetal*, **10**, 22–34.
 - Bijoor NS, Czimczik CI, Pataki DE, Billings SA (2008) Effects of temperature and fertilization on nitrogen cycling and community composition of an urban lawn. *Global Change Biology*, 14, 2119–2131.
 - Blanc-Betes E, Welker JM, Sturchio NC, Chanton JP, Gonzalez-Meler MA (2016) Winter precipitation and snow accumulation drive the methane sink or source strength of Arctic tussock tundra. *Global Change Biology*, 22, 2818–2833.
 - Blüthgen N, Dormann CF, Prati D et al. (2012) A quantitative index of land-use intensity in grasslands: Integrating mowing, grazing and fertilization. *Basic and Applied Ecology*, **13**, 207–220.
 - Bodelier PL., Laanbroek HJ (2004) Nitrogen as a regulatory factor of methane oxidation in soils and sediments. *FEMS Microbiology Ecology*, **47**, 265–277.
 - Butterbach-Bahl K, Baggs EM, Dannenmann M, Kiese R, Zechmeister-Boltenstern S (2013) Nitrous oxide emissions from soils: how well do we understand the processes and their controls? *Philosophical transactions of the Royal Society of London. Series B, Biological sciences*, **368**, 20130122.

Chadwick DR, Pain BF, Brookman SKE (2000) Nitrous Oxide and Methane Emissions following

Application of Animal Manures to Grassland. Journal of Environment Quality, 29, 277–287.

- Chang J, Ciais P, Viovy N, Vuichard N, Sultan B, Soussana J-FF (2015) The greenhouse gas balance of European grasslands. *Global Change Biology*, **21**, 3748–3761.
- Chapuis-Lardy L, Wrage N, Metay A, Chotte JL, Bernoux M (2007) Soils, a sink for N2O? A review. *Global Change Biology*, **13**, 1–17.
- Chiavegato MB, Powers WJ, Carmichael D, Rowntree JE (2015) Pasture-derived greenhouse gas emissions in cow-calf production systems. *Journal of Animal Science*, **93**, 1350.
- Clough TJ, Sherlock RR, Rolston DE (2005) A review of the movement and fate of N₂O in the subsoil. *Nutrient Cycling in Agroecosystems*, **72**, 3–11.
- Conrad R (2009) The global methane cycle: recent advances in understanding the microbial processes involved. *Environmental Microbiology Reports*, **1**, 285–292.
- Cowan NJ, Norman P, Famulari D, Levy PE, Reay DS, Skiba UM (2015) Spatial variability and hotspots of soil N₂O fluxes from intensively grazed grassland. *Biogeosciences*, **12**, 1585–1596.
- Davidson EA (2009) The contribution of manure and fertilizer nitrogen to atmospheric nitrous oxide since 1860. *Nature Geoscience*, **2**, 659–662.
- Dengel S, Levy PE, Grace J, Jones SK, Skiba UM (2011) Methane emissions from sheep pasture, measured with an open-path eddy covariance system. *Global Change Biology*, **17**, 3524– 3533.
- Dengel S, Zona D, Sachs T et al. (2013) Testing the applicability of neural networks as a gapfilling method using CH₄ flux data from high latitude wetlands. *Biogeosciences*, **10**, 8185– 8200.

- Dijkstra FA, Morgan JA, Follett RF, LeCain DR (2013) Climate change reduces the net sink of CH₄ and N₂O in a semiarid grassland. *Global Change Biology*, **19**, 1816–1826.
- Dumortier P, Aubinet M, Beckers Y et al. (2017) Methane balance of an intensively grazed pasture and estimation of the enteric methane emissions from cattle. *Agricultural and Forest Meteorology*, **232**, 527–535.
- Dunfield PF (2007) The soil methane sink. In: *Greenhouse gas sinks* (eds Reay DS, Hewitt CN, Smith KA, Grace J), pp. 152–170. CABI, Wallingford.
- Dutaur L, Verchot L V. (2007) A global inventory of the soil CH₄ sink. *Global Biogeochemical Cycles*, **21**, GB4013.
- Eugster W, Merbold L (2015) Eddy covariance for quantifying trace gas fluxes from soils. *Soil*, **1**, 187–205.

FAOSTAT (2017) Food and Agriculture Organization Corporate Statistical Database.

- Felber R, Neftel A, Ammann C, Münger A, Neftel A, Ammann C (2015) Eddy covariance methane flux measurements over a grazed pasture: effect of cows as moving point sources. *Biogeosciences*, **12**, 3925–3940.
- Firestone MK, Davidson EA (1989) Microbiologial basis of NO and N₂O production and consumption in soil. In: *Exchange of trace gases between terrestrial ecosystems and the atmosphere* (eds Andreae MO, Schimel DS), pp. 7–21. John Wiley & Sons, New York.
- Fowler D, Pilegaard K, Sutton MA et al. (2009) Atmospheric composition change: Ecosystems-Atmosphere interactions. *Atmospheric Environment*, **43**, 5193–5267.
- Frankenberg C, Aben I, Bergamaschi P et al. (2011) Global column-averaged methane mixing ratios from 2003 to 2009 as derived from SCIAMACHY: Trends and variability. *Journal of*

Geophysical Research: Atmospheres, **116**, 1–12.

Galloway JN, Aber JD, Erisman JW et al. (2003) The nitrogen cascade. *BioScience*, 53, 341.

- Gelfand I, Zenone T, Jasrotia P, Chen J, Hamilton SK, Robertson GP (2011) Carbon debt of Conservation Reserve Program (CRP) grasslands converted to bioenergy production. *Proceedings of the National Academy of Sciences*, **108**, 13864–13869.
- Gilmanov TG, Soussana JF, Aires L et al. (2007) Partitioning European grassland net ecosystem CO₂ exchange into gross primary productivity and ecosystem respiration using light response function analysis. *Agriculture, Ecosystems & Environment*, **121**, 93–120.
- Gilmanov TG, Aires L, Barcza Z et al. (2010) Productivity, respiration, and light-response parameters of world grassland and agroecosystems derived from flux-tower measurements. *Rangeland Ecology & Management*, **63**, 16–39.
- Gomez-Casanovas N, Hudiburg TW, Bernacchi CJ, Parton WJ, DeLucia EH (2016) Nitrogen deposition and greenhouse gas emissions from grasslands: uncertainties and future directions. *Global Change Biology*, 22, 1348–1360.
- Hernandez ME, Marín-Muñiz JL, Moreno-Casasola P, Vázquez V (2014) Comparing soil carbon pools and carbon gas fluxes in coastal forested wetlands and flooded grasslands in Veracruz, Mexico. *International Journal of Biodiversity Science, Ecosystem Services & Management*, 1–12.
- Hiller RV, Bretscher D, DelSontro T et al. (2014) Anthropogenic and natural methane fluxes in Switzerland synthesized within a spatially explicit inventory. *Biogeosciences*, **11**, 1941–1959.

Hofmann K, Farbmacher S, Illmer P (2016) Methane flux in montane and subalpine soils of the

Central and Northern Alps. *Geoderma*, **281**, 83–89.

- Holtan-Hartwig L, Dörsch P, Bakken LR (2002) Low temperature control of soil denitrifying communities: Kinetics of N₂O production and reduction. *Soil Biology and Biochemistry*, 34, 1797–1806.
- Hörtnagl L, Wohlfahrt G (2014) Methane and nitrous oxide exchange over a managed hay meadow. *Biogeosciences*, **11**, 7219–7236.
- Hu Y, Chang X, Lin X et al. (2010) Effects of warming and grazing on N₂O fluxes in an alpine meadow ecosystem on the Tibetan plateau. *Soil Biology and Biochemistry*, **42**, 944–952.
- Huber R, Rigling A, Bebi P et al. (2013) Sustainable Land Use in Mountain Regions Under Global Change: Synthesis Across Scales and Disciplines. *Ecology and Society*, 18, art36.
- Huber R, Briner S, Bugmann H et al. (2014) Inter- and transdisciplinary perspective on the integration of ecological processes into ecosystem services analysis in a mountain region. *Ecological Processes*, **3**, 9.
- Hunter JD (2007) Matplotlib: A 2D Graphics Environment. *Computing in Science* & *Engineering*, **9**, 90–95.
- Imer D, Merbold L, Eugster W, Buchmann N (2013) Temporal and spatial variations of soil CO₂, CH₄ and N₂O fluxes at three differently managed grasslands. *Biogeosciences*, **10**, 5931– 5945.
- IPCC (2006) 2006 IPCC guidelines for national greenhouse gas inventories, Volume 4: Agriculture, forestry and other land use. In: *IPCC national greenhouse gas inventories programme* (eds Eggleston HS, Buendia L, Miwa K, Ngara T, Tanabe K). IGES, Japan, Hayama, Japan.

IPCC (2013) Climate Change 2013: The Physical Science Basis. Contribution of Working Group I to the Fifth Assessment Report of the Intergovernmental Panel on Climate Change (eds Stocker TF, Qin D, Plattner G-K, Tignor M, Allen SK, Boschung J, Nauels A, Xia Y, Bex V, Midgley PM). Cambridge University Press, Cambridge, 1535pp pp.

- Jones SK, Famulari D, Di Marco CF, Nemitz E, Skiba UM, Rees RM, Sutton MA (2011) Nitrous oxide emissions from managed grassland: A comparison of eddy covariance and static chamber measurements. *Atmospheric Measurement Techniques*, **4**, 2179–2194.
- Jones CM, Spor A, Brennan FP et al. (2014) Recently identified microbial guild mediates soil N₂O sink capacity. *Nature Climate Change*, **4**, 801–805.
- Kim Y, Tanaka N (2015) Fluxes of CO₂, N₂O and CH₄ by ²²²Rn and chamber methods in coldtemperate grassland soil, northern Japan. *Soil Science and Plant Nutrition*, **61**, 88–97.
- Klumpp K, Bloor JMG, Ambus P, Soussana JF (2011) Effects of clover density on N₂O emissions and plant-soil N transfers in a fertilised upland pasture. *Plant and Soil*, **343**, 97–107.
- Kroon PS, Schrier-Uijl AP, Hensen A, Veenendaal EM, Jonker HJJ (2010) Annual balances of CH₄ and N₂O from a managed fen meadow using eddy covariance flux measurements. *European Journal of Soil Science*, **61**, 773–784.
- Lal R (2010) Managing Soils and Ecosystems for Mitigating Anthropogenic Carbon Emissions and Advancing Global Food Security. *BioScience*, **60**, 708–721.
- Laville P, Lehuger S, Loubet B, Chaumartin F, Cellier P (2011) Effect of management, climate and soil conditions on N₂O and NO emissions from an arable crop rotation using high temporal resolution measurements. *Agricultural and Forest Meteorology*, **151**, 228–240.

Peichl M, Sonnentag O, Wohlfahrt G et al. (2013) Convergence of potential net ecosystem production among contrasting C₃ grasslands (ed Hooper D). *Ecology Letters*, **16**, 502–512.

- Li C, Frolking S, Frolking TA, Changsheng L, Frolking S, Frolking TA (1992) A model of nitrous oxide evolution from soil driven by rainfall events: 2. Model applications. *Journal of Geophysical Research*, 97, 9759–9776.
- Li Y, Dong S, Liu S et al. (2015) Seasonal changes of CO₂, CH₄ and N₂O fluxes in different types of alpine grassland in the Qinghai-Tibetan Plateau of China. *Soil Biology and Biochemistry*, **80**, 306–314.
- Liu L, Greaver TL (2009) A review of nitrogen enrichment effects on three biogenic GHGs: The CO₂ sink may be largely offset by stimulated N₂O and CH₄ emission. *Ecology Letters*, **12**, 1103–1117.
- Lu H (2016) *The influence of land management and simulated climate change on* N₂O *and* CH₄ *exchange of montane grassland soils.* PhD thesis, University of Freiburg, 126 pp.
- Luo GJ, Kiese R, Wolf B, Butterbach-Bahl K (2013) Effects of soil temperature and moisture on methane uptake and nitrous oxide emissions across three different ecosystem types.
 Biogeosciences, 10, 3205–3219.
- Lüscher A, Mueller-Harvey I, Soussana JF, Rees RM, Peyraud JL (2014) Potential of legumebased grassland-livestock systems in Europe: a review. *Grass and Forage Science*, **69**, 206– 228.
- Luyssaert S, Jammet M, Stoy PC et al. (2014) Land management and land-cover change have impacts of similar magnitude on surface temperature. *Nature Climate Change*, **4**, 389–393.

- Martin C, Morgavi DP, Doreau M (2010) Methane mitigation in ruminants: from microbe to the farm scale. *Animal*, **4**, 351–365.
- McKinney W (2010) Data Structures for Statistical Computing in Python (eds van der Walt S, Millman J). *Proceedings of the 9th Python in Science Conference*, **1697900**, 51–56.
- Le Mer J, Roger P (2001) Production, oxidation, emission and consumption of methane by soils: A review. *European Journal of Soil Biology*, **37**, 25–50.
- Merbold L, Steinlin C, Hagedorn F (2013) Winter greenhouse gas fluxes (CO₂, CH₄ and N₂O) from a subalpine grassland. *Biogeosciences*, **10**, 3185–3203.
- Merbold L, Eugster W, Stieger J, Zahniser M, Nelson D, Buchmann N (2014) Greenhouse gas budget (CO₂, CH₄ and N₂O) of intensively managed grassland following restoration. *Global Change Biology*, **20**, 1913–1928.
- Mishurov M, Kiely G (2010) Nitrous oxide flux dynamics of grassland undergoing afforestation. *Agriculture, Ecosystems and Environment*, **139**, 59–65.
- Mishurov M, Kiely G (2011) Gap-filling techniques for the annual sums of nitrous oxide fluxes. *Agricultural and Forest Meteorology*, **151**, 1763–1767.
- Mori A, Hojito M (2015) Effect of dairy manure type and supplemental synthetic fertilizer on methane and nitrous oxide emissions from a grassland in Nasu, Japan. *Soil Science and Plant Nutrition*, **61**, 347–358.
- Neftel A, Ammann C, Fischer C et al. (2010) N₂O exchange over managed grassland: Application of a quantum cascade laser spectrometer for micrometeorological flux measurements. *Agricultural and Forest Meteorology*, **150**, 775–785.

Paustian K, Lehmann J, Ogle S, Reay D, Robertson GP, Smith P (2016) Climate-smart soils.

Nature, **532**, 49–57.

- Price SJ, Kelliher FM, Sherlock RR, Tate KR, Condron LM (2004) Environmental and chemical factors regulating methane oxidation in a New Zealand forest soil. *Australian Journal of Soil Research*, 42, 767.
 - Reay DS, Davidson EA, Smith KA, Smith P, Melillo JM, Dentener F, Crutzen PJ (2012) Global agriculture and nitrous oxide emissions. *Nature Climate Change*, **2**, 410–416.
 - Reichstein M, Falge E, Baldocchi D et al. (2005) On the separation of net ecosystem exchange into assimilation and ecosystem respiration: review and improved algorithm. *Global Change Biology*, **11**, 1424–1439.
 - Risk N, Snider D, Wagner-Riddle C (2013) Mechanisms leading to enhanced soil nitrous oxide fluxes induced by freeze-thaw cycles. *Canadian Journal of Soil Science*, **93**, 401–414.
 - Rowlings DW, Grace PR, Scheer C, Liu S (2015) Rainfall variability drives interannual variation in N₂O emissions from a humid, subtropical pasture. *Science of The Total Environment*, 512–513, 8–18.
- Saggar S, Jha N, Deslippe J et al. (2013) Denitrification and N₂O:N₂ production in temperate
 grasslands: Processes, measurements, modelling and mitigating negative impacts. *Science of The Total Environment*, 465, 173–195.

Schlesinger WH (2013) An estimate of the global sink for nitrous oxide in soils. Global Change Biology, 19, 2929–2931.

Schmitt M, Bahn M, Wohlfahrt G, Tappeiner U, Cernusca A (2010) Land use affects the net ecosystem CO₂ exchange and its components in mountain grasslands. *Biogeosciences*, 7, 2297–2309.

- Schulze ED, Luyssaert S, Ciais P et al. (2009) Importance of methane and nitrous oxide for Europe's terrestrial greenhouse-gas balance. *Nature Geoscience*, **2**, 842–850.
- Seabold S, Perktold J (2010) Statsmodels: econometric and statistical modeling with Python. *Proceedings of the 9th Python in Science Conference*, 57–61.
- Sherlock RR, Sommer SG, Khan RZ et al. (2002) Ammonia, methane, and nitrous oxide emission from pig slurry applied to a pasture in new zealand. *Journal of Environment Quality*, **31**, 1491–1501.
- Skiba U, Drewer J, Tang YS et al. (2009) Biosphere-atmosphere exchange of reactive nitrogen and greenhouse gases at the NitroEurope core flux measurement sites: Measurement strategy and first data sets. *Agriculture, Ecosystems and Environment*, **133**, 139–149.
- Soussana JF, Allard V, Pilegaard K et al. (2007) Full accounting of the greenhouse gas (CO₂, N₂O, CH₄) budget of nine European grassland sites. *Agriculture, Ecosystems and Environment*, **121**, 121–134.
- Syakila A, Kroeze C (2011) The global nitrous oxide budget revisited. *Greenhouse Gas Measurement and Management*, **1**, 17–26.
- Tate KR (2015) Soil methane oxidation and land-use change from process to mitigation. Soil Biology and Biochemistry, 80, 260–272.
- Teepe R, Brumme R, Beese F (2001) Nitrous oxide emissions from soil during freezing and thawing periods. Soil Biology and Biochemistry, 33, 1269–1275.
- Teh YA, Silver WL, Sonnentag O, Detto M, Kelly M, Baldocchi DD (2011) Large greenhouse gas emissions from a temperate peatland pasture. *Ecosystems*, **14**, 311–325.

Treat CC, Wollheim WM, Varner RK, Grandy AS, Talbot J, Frolking S (2014) Temperature and

peat type control CO_2 and CH_4 production in Alaskan permafrost peats. *Global Change Biology*, **20**, 2674–2686.

- Tubiello FN, Salvatore M, Ferrara AF et al. (2015) The Contribution of Agriculture, Forestry and other Land Use activities to Global Warming, 1990-2012. *Global Change Biology*, 21, 2655–2660.
- UNFCCC (2015) Adoption of the Paris Agreement.
- Unteregelsbacher S, Gasche R, Lipp L et al. (2013) Increased methane uptake but unchanged nitrous oxide flux in montane grasslands under simulated climate change conditions. *European Journal of Soil Science*, **64**, 586–596.
- Van Der Walt S, Colbert SC, Varoquaux G (2011) The NumPy array: A structure for efficient numerical computation. *Computing in Science and Engineering*, **13**, 22–30.
- Wang X, Zhang Y, Huang D, Li Z, Zhang X (2015) Methane uptake and emissions in a typical steppe grazing system during the grazing season. *Atmospheric Environment*, **105**, 14–21.
- Wei D, Xu-Ri, Tenzin-Tarchen et al. (2015) Considerable methane uptake by alpine grasslands despite the cold climate: In situ measurements on the central Tibetan Plateau, 2008-2013. *Global Change Biology*, 21, 777–788.
- Wertz S, Goyer C, Zebarth BJ, Burton DL, Tatti E, Chantigny MH, Filion M (2013) Effects of temperatures near the freezing point on N₂O emissions, denitrification and on the abundance and structure of nitrifying and denitrifying soil communities. *FEMS Microbiology Ecology*, 83, 242–254.
- Whalen SC (2005) Biogeochemistry of methane exchange between natural wetlands and the atmosphere. *Environmental Engineering Science*, **22**, 73–94.

- Wohlfahrt G, Anderson-Dunn M, Bahn M et al. (2008a) Biotic, abiotic, and management controls
 on the net ecosystem CO₂ exchange of European mountain grassland ecosystems. *Ecosystems*, **11**, 1338–1351.
- Wohlfahrt G, Hammerle A, Haslwanter A, Bahn M, Tappeiner U, Cernusca A (2008b) Seasonal and inter-annual variability of the net ecosystem CO₂ exchange of a temperate mountain grassland: Effects of weather and management. *Journal of Geophysical Research: Atmospheres*, **113**, 1–14.
- Wolf B, Zheng X, Brüggemann N et al. (2010) Grazing-induced reduction of natural nitrous oxide release from continental steppe. *Nature*, **464**, 881–884.
- Wu D, Dong W, Oenema O, Wang Y, Trebs I, Hu C (2013) N₂O consumption by low-nitrogen soil and its regulation by water and oxygen. *Soil Biology and Biochemistry*, **60**, 165–172.
- Yvon-Durocher G, Allen AP, Bastviken D et al. (2014) Methane fluxes show consistent temperature dependence across microbial to ecosystem scales. *Nature*, **507**, 488–91.
- Zeeman MJ, Mauder M, Steinbrecher R, Heidbach K, Eckart E, Schmid HP (2017) Reduced snow cover affects productivity of upland temperate grasslands. *Agricultural and Forest Meteorology*, 232, 514–526.
- Zhu R, Sun L, Ding W (2005) Nitrous oxide emissions from tundra soil and snowpack in the maritime Antarctic. *Chemosphere*, **59**, 1667–1675.

Tables

Table 1 Basic information for each research site included in this study.

Site	CH-AWS	AT-STU-P	AT-STU-M	FR-LAQ-I	FR-LAQ-E
Location	Alp Weissenstein, Switzerland 46° 34′ 59″ N	Stubai Valley, Austria 47° 12' 87" N	Stubai Valley, Austria 47° 12' 88" N	Laqueuille, France 45° 38' 00" N	Laqueuille, France 45° 38' 00" N
Latitude					
Longitude	9° 47′ 25″ E	11° 30′ 33″ E	11° 30′ 58″ E	2° 44′ 00″ E	2° 44′ 00″ E
Elevation (m)	1978	1870	1820	1040	1040
Management	extensive	extensive	extensive	intensive	extensive
MAT (°C)	-1.4	3.0	3.0	7.0	7.0
MAP (mm)	1214	1097	1097	1200	1200
Snow cover days	166	124	128	25-91	25-91
Grass (%)	95	n.a.	54	69	77
Clover (%)	< 5	n.a.	5	11	4
Grazing days yr ⁻¹	< 20	120	70	142 - 170	142 - 170
Grazing animals d ⁻¹	20 cows	~7 cows, 15 sheep	~7 cows, 15 sheep	9 - 14 cows	7 - 9 cows
Cutting events	0	0	1	0	0
Harvest C / N (kg ha ⁻¹ DW)	0	0	unknown	0	0
Fertilization events	1	1	1	3	0
Organic fertilizer C / N (kg ha ⁻¹ yr ⁻¹)	unknown	1390 / 70 (solid manure)	1390 / 70 (solid manure)	0	0
	0	0	0	214	0
CO ₂ / N ₂ O / CH ₄ flux method	EC / MC / MC	None / MC / MC	MC / MC / MC	EC / AC / EC	EC / AC / none
CO ₂ / N ₂ O / CH ₄ measurement days	339 / 20 / 20	0 / 27 / 26	0 / 51 / 50	1373 / 1123 / 318	863 / 878 / 0
Chamber plots	16	5	5	4	4
GF _{RM} window size (days)	60	60	60	60	60
Reference	Imer et al. (2013)	Schmitt et al. (2010)	Schmitt et al. (2010)	Klumpp <i>et al.</i> (2011a) Allard <i>et al.</i> (2007)	Klumpp <i>et al.</i> (2011a) Allard <i>et al.</i> (2007)

Table 1 Continued.

Site	CH-FRU-I	CH-FRU-E	AT-NEU	DE-GAP
Location	Früebüel, Switzerland	Früebüel, Switzerland	Neustift, Austria	Garmisch-Partenkirchen,
				Germany
Latitude	47° 6′ 57″ N	47° 6′ 57″ N	47° 07′ 00″ N	47° 28' 32.12" N
Longitude	8° 32′ 16″ E	8° 32′ 16″ E	11° 19′ 07″ E	11° 3' 44.47" E
Elevation (m)	982	982	970	734
Management	intensive	extensive	intensive	extensive
MAT (°C)	6.1	6.1	6.5	6.8
MAP (mm)	1682	1682	852	1371
Snow cover days	111	111	93 / 92	72 - 91
Grass (%)	n.a.	n.a.	20-40	52
Clover (%)	5 - 25	5 - 25	5	8
Grazing days yr ⁻¹	29	10	0	0
Grazing animals d ⁻¹	54-57 cows	40-56 cows	0	0
Cutting events	1	2	2010: 3	2012: 3
5			2011: 3	2013: 3
Harvest C / N (kg ha ⁻¹ DW)	1482 / 95	4389 / 280	2010: 3470 / 169	2012: 2940 / 150
			2011: 3676 / 180	2013: 4507 / 245
Fertilization events	3	1	2010: 1	2012: 1
			2011:1	2013: 2
Organic fertilizer C / N (kg ha ⁻¹ yr ⁻¹)	939 / 159 (slurry)	495 / 33 (slurry)	2730 / 341 (solid manure & slurry)	2012: 390 / 61 (slurry)
· · · · ·			× , , , , , , , , , , , , , , , , , , ,	2013: 1071 / 122 (slurry)
Mineral fertilizer N (kg ha ⁻¹ yr ⁻¹)	0	0	0	0
CO ₂ / N ₂ O / CH ₄ flux method	EC / MC / MC	EC / MC / MC	EC / EC / EC	all: MC
$CO_2 / N_2O / CH_4$ measurement days	570 / 35 / 34	571 / 35 / 35	769 / 598 / 596	0/92/93
Chamber plots	6	10	0	3
GF _{RM} window size (days)	15	60	15	120
Reference	Imer et al. (2013)	Imer et al. (2013)	Hörtnagl & Wohlfahrt (2014) Wohlfahrt <i>et al.</i> (2008)	Lu, (2016)

Table 1 Continued.

Site	DE-FEN-I¶	DE-FEN-E¶	CH-CHA-I1	CH-CHA-I2†	CH-CHA§
Location	Fendt, Germany	Fendt, Germany	Chamau, Switzerland	Chamau, Switzerland	Chamau, Switzerland
Latitude	47° 82′ N	47° 82′ N	47° 12′ 37″ N	47° 12′ 37″ N	47° 12′ 37″ N
Longitude	11° 06' E	11° 06′ E	8° 24′ 38″ E	8° 24′ 38″ E	8° 24′ 38″ E
Elevation (m)	600	600	393	393	393
Management	intensive	extensive	intensive	intensive	intensive
MAT (°C)	8.6	8.6	9.1	9.1	9.1
MAP (mm)	933	933	1151	1151	1151
Snow cover days	43 - 54	43 - 54	< 7	< 7	< 7
Grass (%)	42	42	80	80	60
Clover (%)	18 - 26	18 - 26	20	20	40
Grazing days yr ⁻¹	0	0	2010: 0	2010: 50	2012: 7
			2011: 18	2011:18	2013: 1
Grazing animals d ⁻¹	0	0	2010: 0	2010: 40 - 160 sheep	2012: 50 sheep
0			2011: 50 - 60 sheep	2011: 50 - 60 sheep	2013: 70 sheep
Cutting events	2012: 5	2012: 3	2010: 5	2010: 4	2012: 5
C	2013: 4	2013: 3	2011: 5	2011: 5	2013: 5
	2014: 5	2014: 3			
Harvest C / N (kg ha ⁻¹ DW)	2012: 4790 / 389	2012: 4664 / 273	2010: 3449 / 222	2010: 1262 / 81	2012: 1500 / 96
_	2013: 6374 / 420	2013: 4437 / 247	2011: 2468 / 159	2011: 1850 / 119	2013: 4233 / 272
	2014: 5841 / 289	2014: 3989 / 169			
Fertilization events	2012: 5	2012: 1	2010: 5	2010: 5	2012: 6
	2013: 6	2013: 2	2011: 6	2011:6	2013: 4
	2014: 4	2014: 1			
Organic fertilizer C / N (kg ha ⁻¹ yr ⁻¹)	2012: 2204 / 312 (slurry)	2012: 389 / 61 (slurry)	2010: 1426 / 253 (slurry)	2010: 1487 / 194 (slurry)	2012: 2233 / 269 &
	2013: 3310 / 365 (slurry)	2013: 1071 / 122 (slurry)	2011: 1222 / 254 (slurry)	2011: 1510 / 258 (slurry)	2013: 978 / 232 (slurry
	2014: 2503 / 243 (slurry)	2014: 288 / 61 (slurry)			
Mineral fertilizer N (kg ha ⁻¹ yr ⁻¹)	0	0	0	0	2012: 17
					2013: 0
CO ₂ / N ₂ O / CH ₄ flux method	all: MC & AC	all: MC & AC	EC / MC / MC	EC / MC / MC	EC / EC / EC
CO ₂ / N ₂ O / CH ₄ measurement days	1096 / 626 / 629	0 / 659 / 659	676 / 38 / 36	698 / 38 / 37	715 / 694 / 694
Chamber plots	6	6	8	8	0
$\mathbf{GF}_{\mathbf{RM}}$ window size (days)	60	60	30	30	60
Reference	Lu, (2016) Zeeman <i>et al.</i> (2017)	Lu, (2016)	Imer et al. (2013)	Imer et al. (2013)	Merbold et al. (2014)

¶ Grass and clover percentages are given as fraction of total dry weight and is not related to spatial coverage;

[†] CH-CHA-I2 2010: rolling and resowing in March/April, herbicide in July;

§ CH-CHA 2012: ploughing on 2 February, resowing, rolling, harrowing in March and April, herbicide/pesticide in July and September;

& During 2012, solid manure was applied in January, otherwise slurry.

Abbreviations: MAP, mean annual precipitation; MAT, mean annual temperature; DW, dry weight; GF_{RM}, gap-filling with running median;

Flux measurement method: AC, automatic chambers; EC, eddy covariance method; MC, manual chambers;

Table 2 Percentile distribution of measured, non-gapfilled N₂O (F_{N2O}) and CH₄ (F_{CH4}) fluxes, soil temperature (TS) and water-filled pore space (WFPS) for data shown in Figure 3-Figure 5 for each site. P_{zf} corresponds to the zero-flux percentile, i.e. the percentile rank where the flux was found to be zero; P₂₅ and P₇₅ refer to the 25th and 75th percentile, i.e. values in-between give the interquartile range; P₅₀ corresponds to the 50th percentile (median).

		$\mathbf{Flux} \ (\mu \mathbf{g} \ \mathbf{m}^{-2} \ \mathbf{h}^{-1})$				TS (°C)	WFPS (%)			
Site	$\mathbf{P}_{\mathbf{zf}}$	P ₂₅	P ₅₀	P ₇₅	P ₂₅	P ₅₀	P ₇₅	P ₂₅	P ₅₀	P ₇₅	
F _{N2O}											
CH-AWS	0	5	17	73	10	12	12	38	55	64	
STU-P	4	5	6	10	11	12	13	44	51	54	
STU-M	15	4	8	13	9	11	12	59	62	68	
FR-LAQ-I	10	3	12	29	7	12	15	59	63	69	
FR-LAQ-E	9	2	6	13	6	10	14	61	66	70	
CH-FRU-I	2	7	21	33	10	12	14	57	77	82	
CH-FRU-E	0	9	17	23	10	12	14	57	77	82	
AT-NEU	35	-4	4	20	2	11	15	50	61	68	
DE-GAP	15	2	11	22	10	15	20	59	68	71	
DE-FEN-I	5	10	17	41	6	12	18	55	67	71	
DE-FEN-E	4	6	11	21	7	13	18	54	61	65	
CH-CHA-I1	0	18	39	133	12	16	19	64	82	89	
CH-CHA-I2	1	27	56	238	12	16	19	64	82	89	
CH-CHA	12	16	56	264	5	13	18	85	91	94	
Range (min, max)	0, 35	-4, 27	4, 56	10, 264	2, 12	10, 16	12, 20	38, 85	51, 91	54, 94	
F _{CH4}											
CH-AWS	n.a.	-41	-28	-18	10	12	12	38	55	64	
STU-P	85	-40	-29	-18	11	12	14	41	50	54	
STU-M	95	-56	-40	-24	10	11	13	59	62	68	
CH-FRU-I	81	-22	-17	-8	10	12	14	54	77	81	
CH-FRU-E	86	-20	-12	-9	10	12	14	57	77	82	
AT-NEU	27	-6	36	76	2	11	15	50	61	68	
DE-GAP	77	-26	-12	-1	10	15	20	59	68	71	

DE-FEN-I	87	-18	-10	-5	6	12	18	55	67	71
DE-FEN-E	87	-18	-11	-6	7	13	18	54	61	65
CH-CHA-I1	80	-15	-14	-2	13	16	19	63	82	89
CH-CHA-I2	81	-16	-12	-4	12	16	19	64	82	89
CH-CHA	36	-115	111	364	5	13	18	85	91	94
Range (min, max)	27, 95	-115, -6	-40, 111	-24, 364	2, 13	11, 16	12, 20	38, 85	50, 91	54, 94

Table 3 Regression analysis using daily averages with log-transformed CH₄ (F_{CH4}) and N₂O (F_{N2O}) flux rates as dependent variables. Soil temperature (TS) and water-filled pore space (WFPS) were used as driver variables. Before log-transformation, the site-specific minimum flux + 1 was added to observed fluxes. Only background fluxes were included in the regression analysis, time periods in temporal proximity to management events (cutting, fertilization) and periods of snow cover were excluded from the analysis. Linear models: y = ax + by + c for multiple linear regression, y = dx + e for simple linear regression. n, number of available measurement days used in the regression analyses; r_{adj}^2 , coefficient of determination after adjustment based on the degrees of freedom of the respective model; stars indicate significance levels: *, P < 0.05; **, P < 0.01; ***, P < 0.001;

		Multiple linear regression (TS + WFPS) Simple linear regression												
			•	Regressio	n coeffici	ients			Regression	coefficients			Regression coefficients	
Site	Measurement technique	n	$r^2(r^2_{adj})$	c (intercept	a t)(TS)	b (WFPS)	n	$r^2(r^2_{adj})$	e (intercept)	d (TS)	n	$r^2(r^2_{adj})$	e (intercept)	d (WFPS
log(F _{N2O})														
CH-AWS	MC	19	0.31 (0.22)	-0.269	0.011	0.007*	19	0.07 (0.01)	-0.056	0.021	19	0.29 (0.25)*	-0.164	0.007
AT-STU-P	MC	21	0.13 (0.04)	0.024	0.003	0.000	21	0.13 (0.09)	0.032	0.003	21	0.00 (-0.05)	0.072	0.000
AT-STU-M	I MC	18	0.46 (0.38)*	-0.235*	0.010**	0.003*	18	0.24 (0.19)*	0.009	0.008*	18	0.08 (0.02)	-0.035	0.002
FR-LAQ-I	EC	570	0.10 (0.10)***	· -0.213	0.022**	*0.003	684	0.05 (0.05)***	• 0.027	0.013***	570	0.01 (0.01)*	0.422***	-0.004
FR-LAQ-E	AC	591	0.10 (0.09)***	· -0.198	0.021**	*0.002	711	0.05 (0.04)***	• 0.033	0.012***	591	0.01 (0.01)*	0.404***	-0.00
CH-FRU-I	MC	33	0.24 (0.19)*	-0.085	0.010**	0.002*	33	0.11 (0.08)	0.099*	0.006	33	0.01 (-0.02)	0.130*	0.001
CH-FRU-E	MC	27	0.47 (0.43)***	· -0.097	0.012**	*0.001**	27	0.27 (0.24)**	0.029	0.008**	27	0.05 (0.01)	0.095*	0.001
AT-NEU	EC	400	0.14 (0.10)***	• 0.460***	0.003**	-0.002***	400	0.06 (0.06)***	• 0.321***	0.005***	400	0.12 (0.11)***	* 0.513***	-0.00
DE-GAP	MC	59	0.21 (0.18)**	-0.204*	0.005*	0.004***	59	0.01 (-0.01)	0.108**	0.002	67	0.08 (0.06)*	-0.028	0.002
DE-FEN-I	AC	244	0.03 (0.03)*	0.151	0.004	0.000	506	0.08 (0.08)***	• 0.078***	0.006***	244	0.02 (0.02)*	0.306***	-0.00
DE-FEN-E	AC	299	0.02 (0.02)*	-0.013	0.002	0.002*	547	0.01 (0.01)**	0.107***	0.002**	303	0.02 (0.01)*	0.062	0.002
CH-CHA-I	1 MC	31	0.19 (0.13)	-1.135	0.028	0.014*	33	0.02 (-0.02)	0.228	0.009	31	0.08 (0.05)	-0.278	0.008
CH-CHA-I	2MC	54	0.14 (0.10)*	-1.067	0.038**	0.012*	56	0.05 (0.04)	0.121	0.020	54	0.01 (-0.01)	0.168	0.003
CH-CHA	EC	610	0.15 (0.15)***	\$ 3.407***	-0.008*	-0.025***	610	0.02 (0.02)***	* 1.003***	0.010***	610	0.14 (0.14)***	* 2.981***	-0.02
log(F _{CH4})														
	MC	19	0.77 (0.74)***	° 0.047	-0.015	0.009***	19	0.00 (-0.06)	0.304	0.004	19	0.72 (0.71)***	* -0.085	0.00
AT-STU-P	MC	26	0.03 (-0.05)	1.809***	-0.006	0.000	26	0.03 (-0.01)	1.792***	-0.006	26	0.00 (-0.04)	1.717***	0.000
AT-STU-M	I MC	20	0.05 (-0.06)	0.285	0.021	0.004	20	0.05 (-0.01)	0.548*	0.019	20	0.00 (-0.05)	0.687	0.001

	FR-LAQ-I	AC	148	0.24 (0.23)***	0.552	0.182***	*0.011	178	0.24 (0.24)***	1.388***	0.171***	148	0.00 (-0.00)	4.393***	-0.011
1	FR-LAQ-E 1	1.a.	n.a.	n.a.	n.a.	n.a.	n.a.	n.a.	n.a.	n.a.	n.a.	n.a.	n.a.	n.a.	n.a.
	CH-FRU-I	мС	32	0.19 (0.13)	-0.038	0.006	0.004*	32	0.00 (-0.03)	0.363***	-0.003	32	0.16 (0.14)*	0.082	0.004*
	CH-FRU-E I	мс	27	0.40 (0.35)**	0.014	-0.003	0.004**	27	0.11 (0.07)	0.430***	-0.014	27	0.40 (0.37)***	-0.043	0.005***
	AT-NEU I	EC	398	0.04 (0.03)***	1.716***	0.008***	*0.002*	398	0.02 (0.02)**	1.855***	0.006**	398	0.01 (0.00)	1.865***	0.001
	DE-GAP I	мс	58	0.40 (0.37)***	0.280	-0.004	0.010***	58	0.13 (0.12)**	0.988***	-0.011**	68	0.18 (0.16)***	0.282	0.008***
1	DE-FEN-I	AC	244	0.22 (0.21)***	0.185*	0.000	0.005***	509	0.14 (0.14)***	0.599***	-0.007***	244	0.22 (0.22)***	0.196***	0.005***
]	DE-FEN-E	AC	299	0.32 (0.32)***	0.226***	-0.002	0.006***	549	0.16 (0.16)***	0.628***	-0.008***	303	0.30 (0.29)***	0.149***	0.007***
	CH-CHA-III	мс	29	0.10 (0.03)	0.191	-0.006	0.002	31	0.07 (0.04)	0.329***	-0.008	29	0.07 (0.03)	0.002	0.003
	CH-CHA-I2I	мс	54	0.20 (0.17)**	-0.099	0.000	0.004**	55	0.06 (0.04)	0.300***	-0.006	54	0.20 (0.19)***	-0.111	0.004***
	CH-CHA I	EC	609	0.00 (-0.00)	3.154***	0.003	0.000	609	0.00 (0.00)	3.187***	0.002	609	0.00 (-0.00)	3.305***	-0.001

Table 4 Annual cumulative CO_2 , N_2O and CH_4 site budgets, calculated from gap-filled data. For sites where more than one year of measurements were available, multi-year averages \pm the standard error of the mean are given. Net greenhouse gas balance (NGB) is given as the sum of CO_2 flux + N_2O flux + CH_4 flux. CO_2 flux offset represents the percentage of CO_2 uptake that is offset by N_2O and CH_4 fluxes, i.e. corresponds to the ratio between the sum of N_2O flux + CH_4 flux and the CO_2 flux. For NGB and the CO_2 flux offset, numbers are shown in brackets if not all three compounds were measured.

Site	Year	Cun	nulative budg	ets (g CO ₂ -eq. r	$n^{-2} yr^{-1}$)	CO ₂ flux offset
		CO ₂ flux	N ₂ O flux	CH ₄ flux	NGB	
CH-AWS	2010/11	-1783	107	-9	-1685	5%
AT-STU-P	2011	n.a.	18	-7	(11)	n.a.
AT-STU-M	2011	n.a.	20	-9	(11)	n.a.
FR-LAQ-I	2008	-1537	93	n.a.	(-1444)	(6%)
	2009	-1444	247	n.a.	(-1197)	(17%)
	2010	-814	48	388	-378	54%
	2011	-1019	68	588	-363	64%
	2012	n.a.	56	n.a.	(56)	n.a.
	2013	n.a.	25	n.a.	(25)	n.a.
	2008-2013	-1204 ± 172	90 ± 33	488 ± 100	-626	48%
FR-LAQ-E	2008	-1276	17	n.a.	(-1259)	(1%)
	2009	-657	30	n.a.	(-627)	(5%)
	2010	-916	20	n.a.	(-897)	(2%)
	2011	n.a.	23	n.a.	(23)	n.a.
	2012	n.a.	16	n.a.	(16)	n.a.
	2013	n.a.	10	n.a.	(10)	n.a.
	2008-2013	-950 ± 179	19 ± 3	n.a.	(-931)	(2%)
CH-FRU-I	2010/11	-2806	47	-2	-2761	2%

CH-FRU-E	2010/11	-1371	40	-4	-1335	3%
AT-NEU	2010	-111	10	14	-87	22%
	2011	-70	30	11	-29	59%
	2010-2011	-91 ± 20	20 ± 10	13 ± 2	-58	36%
DE-GAP	2012	n.a.	25	1	(26)	n.a.
	2013	n.a.	27	-3	(24)	n.a.
	2012-2013	n.a.	26 ± 1	-1 ± 2	(25)	n.a.
DE-FEN-I	2012	-737	101	9	-627	15%
	2013	-954	57	1	-896	6%
	2014	-1238	37	-1	-1202	3%
	2012-2014	-976 ± 145	65 ± 19	3 ± 3	-909	7%
DE-FEN-E	2012	n.a.	38	4	(42)	n.a.
	2013	n.a.	52	-3	(49)	n.a.
	2014	n.a.	36	-3	(33)	n.a.
	2012-2014	n.a.	42 ± 5	-1 ± 2	(41)	n.a.
CH-CHA-I1	2010/11	-2403	245	-2	-2160	10%
CH-CHA-I2	2010/11	-912	370	-2	-544	40%
CH-CHA	2012§	1246	1157	43	2446	-96%
	2013	-4671	119	38	-4514	3%
	2012-2013	-1713 ± 2959	638 ± 519	41 ± 3	-1034	40%
Mean across site	es					$21\pm6\%$

§ CH-CHA 2012: year of grassland restoration (including ploughing)

									N ₂ O			CH ₄	
ID Site	Reference	Years	Time	Method	Sampling freq.	Management	Min	Max	Mean ± SEM	Min	Max	Mean ± SEM	Notes
1 CH-AWS	this study	2010/11	YR	MC	~WK	G, (F)	0 DY	181 DY	41 YR	-57 DY	-15 DY	-30 YR	¶
	this study	2011	GWS	MC	WK	G, F	-5 DY	22 DY	7 ^{DY}	-86 DY	75 ^{DY}	-23 ^{DY}	¶
	this study	2011	GWS	MC	WK	G, C, F	-8 DY	26 ^{DY}	8	-114 DY	49 ^{DY}	-32	1
4 FR-LAQ-I	this study	CH ₄ : 2010-2011, N ₂ O: 2008-	CH ₄ : GWS, N ₂ O:	CH4: EC, N2O: AC	DY	G, F	-94 ^{DY}	1298	34 ± 13 YR	-206 DY	12459 ^{DY}	$1639\pm336~^{\rm DY}$	cows in fo
		2013	YR			_	DV	DY	VP				
5 FR-LAQ-E	this study	2008-2013	YR	AC	DY	G	-32 DY	199 ^{DY}	7 ± 1 YR	DV	DV		_
	this study	2010/11	YR	MC	~WK	G, C, F	-7 ^{DY}	126 DY	18	-37 DY	63 DY	-6	1
	this study	2010/11	YR	MC	~WK	G, C, F	0 ^{DY}	282 DY	15 	-57 ^{DY}	24 DY	-12	1
8 AT-NEU	this study	2011	YR	EC	20 Hz	C, F	-277 DY	121 DY	8 ± 4 YR	-1911 _{DY}	602 ^{DY}	$41 \pm 5^{\text{YR}}$	
9 DE-GAP	this study	2012-2013	YR	MC	WK	C, F	-11 DY	127 ^{DY}	$10\pm0~^{\rm YR}$	-70 ^{DY}	404 ^{DY}	-4 ± 7 YR	
10 DE-FEN-I	this study	2012-2013	YR	AC	DY	C, F	-8 ^{DY}	2055	25 ± 7 YR	-57 ^{DY}	6377 ^{DY}	$11 \pm 10^{\text{YR}}$	
								DY					
11 DE-FEN-E	this study	2012-2014	YR	AC	DY	C, F	-8 DY	366 DY	$16 \pm 2^{\text{YR}}$	-54 DY	8907 DY	-2 ± 8 YR	_
	this study	2010/11	YR	MC	~WK	G, C, F	-1 DY	849 ^{DY}	94	-23 DY	111 ^{DY}	-5	٩
13 CH-CHA-I2	this study	2010/11	YR	MC	~WK	G, C, F	-4 ^{DY}	1529 DY	142	-28 DY	20 ^{DY}	-6	¶
14 CH-CHA	this study	2012-2013	YR	EC	20 Hz	G, C, F	-803	4868	244 ± 199	-1327 DY	4234 ^{DY}	136 ± 8	2012: gras
15 Janon Marris Pr	Welf	2007/2008	VD	10	> DV		dy -8 SM	_{DY} 75 SM	4	Di			restoration
15 Inner Mongolia	Wolf et al. (2010)	2007/2008	YR GZS	AC	>DY	none	-8 ^{0M}	5 ^{ww}	$4 2 \pm 2^{YR}$	-45 ^{ww}	0^{WW}	-23 ± 23 YR	steppe gra
16 LCRC, USA	Chiavegato et al. (2015)			MC	DY	none	-9 SM	5 п.п. 31 SM	2 ± 2^{-1}	-45	0	-23 ± 23	*,¶
17 Inner Mongolia	Wolf et al. (2010)	2007/2008	YR	AC	>DY	G	-9 *** 7 ^{WW}	64 ^{WW}	0 41 ± 17 ^{YR}	-35 ^{ww}	145 ^{ww}	48 ± 52 YR	steppe gra
18 LCRC, USA	Chiavegato et al. (2015)		GZS GZS	MC MC	DY DY	G G	6 ^{ww}	64 83 ^{ww}	41 ± 17 $39 \pm 23^{\text{YR}}$	-35 -55 ^{WW}	145 125 ^{ww}	48 ± 52 43 ± 53 YR	¶, *, irriga ¶ *
19 LCRC, USA 20 Estero Dulce, MX	Chiavegato et al. (2015) Hernandez et al. (2014)		YR	MC	bi-MN	G	0	65	59 ± 25	-33 6070 ^{DS}	125	45 ± 55 116760 ^{YR}	¶, flooded
	Hernandez <i>et al.</i> (2014) Hernandez <i>et al.</i> (2014)	2010-2012	IK	MC	DI-IVIIN	0				0070	181210 RS	110700	¶, nooded
21 Nam Co, CN	Wei et al. (2014)	2009-2013	GWS	MC	WK	G				-96 YR	-49 ^{YR}	$-72\pm3~^{\rm YR}$	¶, steppe
22 Nam Co, CN	Wei et al. (2014)	2012-2013	GWS	MC	WK	G				-74 ^{YR}	-37 ^{YR}	-59 ± 4 ^{YR}	¶, meadov
23 Bugac, HU	Soussana et al. (2007)	2002-2004	YR	CH4: EST, N2O: MC,		G	15^{YR}	18^{YR}	17 ± 1 YR	117 ^{YR}	218 YR	167 ± 50 YR	Ť
				TDL		_		- VD	VD		- · · · VD	ND ND	
24 Laqueuille, FR (E)	Soussana et al. (2007)	2002-2004	YR	CH4: SF6, N2O: MC, TDL		G	3 YR	3 ^{YR}	$3\pm0^{~\rm YR}$	636 ^{yr}	719 ^{yr}	$678 \pm 42 \ ^{\rm YR}$	Ť
25 Haibei, CN	Li et al. (2015)	2013	GWS	MC	DY	G	-2 ^{MN}	9^{MN}	4 ± 3 ^{MN}	-17 ^{MN}	13 ^{MN}	2 ± 9 ^{MN}	¶, #, alpin
26 Haibei, CN	Li et al. (2015)	2013	GWS	MC	DY	G	-1 ^{MN}	11 ^{MN}	5 ± 3 ^{MN}	-2 ^{MN}	25 ^{MN}	12 ± 8^{MN}	¶, #, alpin
27 MUDF4, NZ	Bhandral et al. (2010)	2003/04	GWS, WIN	MC	DY	G	98 ^{DY}	1074 ^{DY}	301 ± 40				\$
28 Easter Bush, GB	Dengel et al. (2011)	2010	GWS	EC	20 Hz	G				0^{DY}	4167 ^{DY}	1043 ^{DY}	sheep past
29 Sherman Island, US	Baldocchi et al. (2012)	2007-2010	GWS	EC	10 Hz	G						1320 ± 1014 Y	R peatland p
30 Dorinne, BE	Dumortier et al. (2017)	2013	YR	EC	10 Hz	G				63	14554	1107 YR	&, cattle p
	Rowlings et al. (2015)	2007-2008	YR	AC	DY	G	1^{DY}	761 $^{\rm DY}$	$31\pm8~^{\rm YR}$				subtropica
NZ 32 Oensingen, CH (E)	Soussana et al. (2007)	2002-2004	YR	MC, TDL		С	-4 ^{YR}	-4^{YR}	$-4\pm0^{~\rm YR}$				
33 Sapporo, JP	Kim & Tanaka (2015)	1996/97	GWS, WIN	MC, IDL MC	>=MN	č	4 DY	14 ^{DY}	8 ^{SUM} /13 ^{WIN}	-24 ^{DY}	0 DY	$-10^{\text{SUM}}/0^{\text{WIN}}$	
34 Dümmer peatland, DE		2007-2011	YR	MC	bi-WK	Č	0 YR	2 YR	10 ± 7 YR	-47 YR	48 YR	-14 ± 8 SEM	
	• • •											YR	
35 Nasu, JP	Mori & Hojito (2014)	2008-2010	YR	MC	~WK	C, F	-26 DY	111 DY	10 ± 4 YR	-173 DY	167 ^{DY}	-18 ± 0 YR	F: PK
36 Nasu, JP	Mori & Hojito (2014)	2008-2010	YR	MC	~WK	C, F	-33 DY	1493 DY	$84 \pm 37 \frac{\text{YR}}{\text{YR}}$	-173 DY	3028 DY	$16 \pm 9 \frac{\text{YR}}{\text{YR}}$	F: SL, PK
37 Nasu, JP	Mori & Hojito (2014)	2008-2010	YR	MC	~WK	C, F	-13 ^{DY}		$88 \pm 34^{\text{YR}}$	-156 ^{DY}	334 ^{DY}	-15 \pm 8 $^{\rm YR}$	F: MA, PF
	Soussana et al. (2007)	2002-2004	YR	MC, TDL		C, F	19 YR	35 YR	$27 \pm 8 \frac{\text{YR}}{\text{YR}}$				
39 Lille Valby, DK	Soussana et al. (2007)	2002-2004	YR	MC, TDL		C, F	5 YR	14 YR	$10 \pm 4^{\text{YR}}$		VD		_
40 Oukoop, NL	Kroon et al. (2010b)	2006-2008	YR	EC, QCL		C, F	274 ^{YR}		274 YR	1701 ^{YR}	2009 YR	1884 ^{YR}	fen meado
41 Edinburgh, GB	Cowan et al. (2015)	2013	SUM	MC	>DY	G, F	11	7022	47 ^{DY}			VD	§, sheep
	Teh et al. (2011)	2007/08	YR	EC	10 Hz	G, F			100			312 YR	peatland p
43 Sherman Island, US	Teh et al. (2011)	2007/08	YR	MC	WK	G, F	196 ^{DY}	7397 dy	419 YR			1436 ^{YR}	¶, peatland
44 Laqueuille, FR (I)	Soussana et al. (2007)	2002-2004	YR	CH4: SF6, N2O: MC,		G, F	12^{YR}	14^{YR}	$13\pm1^{~\rm YR}$	1255 ^{YR}	1322 ^{yr}	$1288\pm33^{\rm YR}$	Ť
45 Malga Arpaco, IT	Soussana et al. (2007)	2002-2004	YR	TDL CH4: EST, N2O: MC,		G, F	0 YR	0 YR	0 YR	301 ^{yr}	301 ^{YR}	$301\pm0^{~\rm YR}$	*
				TDL			-		0	501	501	501 ± 0	1
	Jones et al. (2011)	2003/07/08	GWS	MC		G, F	128 CP	876 ^{CP}	415 ± 120 CP				**
47 Easter Bush, GB	Jones et al. (2011)	2003/07/08	GWS	EC		G, F	69 ^{CP}	1472 CF	411 ± 196 CP				**
48 MUDF4, NZ	vones er un (2011)	2003/04	GWS, WIN	MC	DY	0,1	0,		631 ± 109				

									DY					
	49 Donoughmore, IE	Mishurov & Kiely (2010)	2004-2008	YR	EC	10 Hz	G, C, F	-28 ^{MN}	$503 ^{\text{MN}}$	$86\pm9~^{YR}$				F: SL, MF
	50 Easter Bush, GB	Soussana et al. (2007)	2002-2004	YR	CH4: SF6, N2O: MC, TDL		G, C, F	10 ^{YR}	41 ^{YR}	$26\pm15~^{\rm YR}$	686 ^{YR}	820^{YR}	$753\pm67^{~YR}$	Ť
	51 Carlow, IE	Soussana et al. (2007)	2002-2004	YR	CH4: SF6, N2O: MC, TDL		G, C, F	1 ^{YR}	20^{YR}	$11\pm10^{~\rm YR}$	5357 ^{YR}	703 ^{YR}	$619\pm84~^{\rm YR}$	†
5	52 Lelystad, NL	Soussana et al. (2007)	2002-2004	YR	CH4: SF6, N2O: MC, TDL		G, C, F	50 ^{YR}	122 ^{YR}	$86\pm36^{~YR}$	586 ^{YR}	1456 ^{YR}	$1021\pm435~^{\rm YR}$	†
	53 Dischma Valley, CH	· · · · ·	2010, 2011 (Nov – Apr)	WIN	SP	WK	G, C, F	3 ^{MN}	70^{MN}	36 ^{WIN}	-13 ^{MN}	-5 ^{MN}	-8 ^{WIN}	1

¶ Methane emissions from enteric fermentation not included.

* Measurements were only carried out during a 14d time span after grazing.

 \dagger CH₄ fluxes include only enteric fermentation measured either using the SF₆ tracer technique or estimated using a CH₄ emission rate (see equation 1 in Soussana *et al.* (2007)).

Measurements in May, August and October.

\$ Measurements were only carried during a 14-17d time span after two fertilization events in January and September. Mean: per fertilizer application.

& Minimum value: cattle-free pasture; maximum value: cattle confined to flux footprint area.

§ Dataset: 3d. Measurements were carried out between 10a.m. and 4p.m. GMT. Maximum: manure perimeter.

** The study investigated fluxes during six comparison periods, covering the months of March – July. Each comparison period lasted between 2 and 28d.

Abbreviations: ID, identification number for text references; Sites: E, extensive management; I, intensive management; LCRC, Michigan State Univ. Lake City AgBioResearch Center; MUDF4, Massey Univ. N° 4 Dairy Farm; Method: AC, automatic chambers; EC, eddy covariance method; EST, estimated (see †); MC, manual chambers; SF6, SF6 tracer technique; SP, snow profile method; TDL, tunable diode laser method; Sampling frequency or averaging time: CP, mean over comparison period, see notes; DS, dry season mean; DY, daily; GWS, growing season; GZS, grazing season; MN, monthly; MS, multi-site mean; SEM, standard error of monthly or yearly mean; SM, single measurement mean from three chambers; SUM, summer; WIN, winter; WK, weekly; WW, mean over two weeks; YR, year-round or yearly mean; Management: C, cutting; F, fertilization; (F), amount of fertilizer unknown; G, grazing; Notes: MA, manure; MF, mineral fertilizer; PK, synthetic P and K fertilizers; SL, slurry;

Table 6 N_2O emission factors for fertilized sites with known amount of applied fertilizer in this study. Cumulative N_2O emissions for each site were calculated from complete time series after gap-filling via the running median method. For sites with measurements spanning over multiple years, the site mean was calculated as the mean of the respective annual values \pm the standard error of the mean. The site CH-AWS was not included in this table because the amount of applied fertilizer was unknown.

Site	Year	Available data (days)	Cumulative N ₂ O emissions (kg N ha ⁻¹)	Organic fertilizer input (kg N ha ⁻¹)	Mineral fertilizer input (kg N ha ⁻¹)	Emission factor (%)
CH-FRU-I	2010/11	35	1.02	159	0	0.6
CH-FRU-E	2010/11	35	0.83	33	0	2.5
AT-NEU	2010	215	0.19	341	0	0.1
	2011	296	0.64	341	0	0.2
	site mean	256 ± 41	0.41 ± 0.22	341	0	0.1 ± 0.1
FR-LAQ-I	2008	185	1.97	0	214	0.9
	2009	103	5.28	0	214	2.5
	2010	258	1.02	0	214	0.5
	2011	195	1.46	0	214	0.7
	2012	198	1.21	0	214	0.6
	2013	184	0.57	0	214	0.3
	site mean	187 ± 20	1.92 ± 0.70	0	214	0.9 ± 0.8
DE-GAP	2012	37	0.51	61	0	0.8
	2013	55	0.57	122	0	0.5
	site mean	46 ± 9	0.54 ± 0.03	92 ± 31	0	0.7 ± 0.2
DE-FEN-I	2012	128	2.16	312	0	0.7
	2013	202	1.21	365	0	0.3
	2014	296	0.76	243	0	0.3
	site mean	209 ± 49	1.38 ± 0.41	307 ± 35	0	0.4 ± 0.1
DE-FEN-E	2012	127	0.83	61	0	1.4
	2013	236	1.08	122	0	0.9
	2014	296	0.76	61	0	1.2
	site mean	220 ± 49	0.89 ± 0.10	81 ± 20	0	1.2 ± 0.1
CH-CHA-I1	2010/11	38	5.22	190	0	2.7
CH-CHA-I2	2010/11	38	7.89	219	0	3.6
CH-CHA	2012	328	24.70	269	17	8.6
	2013	360	2.55	232	0	1.1
	site mean	344 ± 16	13.62 ± 11.07	251 ± 19	9 ± 9	4.9 ± 2.2
Mean across sites ± SEM						1.8 ± 0.5

Figure 1 Time periods, measurement techniques and number of available days with measurements of CO_2 , N_2O and CH_4 fluxes. The order of sites from top to bottom follows the elevational gradient, with the highest site listed first. Numbers in brackets refer to the number of chamber replicates. See Table 1 for site name abbreviations. AC, automatic chambers; EC, eddy covariance; MC, manual chambers.

Figure 2 Boxplots of measured, non-gapfilled CO₂, N₂O, and CH₄ fluxes. Note the axis break in the N₂O and CH₄ panels. The order of the sites from left to right follows the elevational gradient, starting with the highest elevation site on the left. Colored boxes show the interquartile range (IQR = Q3 – Q1) of measured data at the respective site, black solid lines inside the colored boxes correspond to the median value. Whiskers extending from the boxes show the range of non-outlier data, defined as Q3 + 1.5 IQR for the upper limit, and as Q1 – 1.5 IQR for the lower limit. Data points beyond the whiskers are considered outliers and plotted as individual points. Colors show the season of the year: spring (March – May, green), summer (June – August, red), autumn (September – November, orange) and winter (December – February, blue). See Table 1 for site name abbreviations.

Figure 3 Hexbin plots of measured, non-gapfilled N_2O fluxes in twelve combined classes of soil temperature and water-filled pore space. Prior to analysis, daily average values of all three variables at each site were converted to an index in the range 0 to 100%, based on the cumulative empirical probability density function (cePDF) of each variable at each site, i.e. the index corresponds with the percentile value of the original measurements in relation to the site-specific cePDF. Colored (red-to-blue gradient) hexbins show the percentile N_2O flux in the respective combined class, while white hexbins show the lack of measurements. (a) Aggregated N_2O flux

percentile values for each site, showing the median of each percentile flux within each aggregation unit. Black dots in hexbins indicate that the respective median percentile flux corresponds to N_2O uptake, while the absence of black dots indicates N_2O emission. The order of sites from left to right and from top to bottom follows the elevational gradient, with results for the highest site shown at the top left. (b) Aggregated N_2O flux percentile values across all sites, calculated as the median of site-level hexbin values in (a), when data from at least two sites were available for a specific combined class. Additional information on percentile distributions at each site is given in Table 2. See Table 1 for site name abbreviations.

Figure 4 Hexbin plots of measured, non-gapfilled CH₄ fluxes in twelve combined classes of soil temperature and water-filled pore space. Prior to analysis, daily average values of all three variables at each site were converted to an index in the range 0 to 100%, based on the cumulative empirical probability density function (cePDF) of each variable at each site, i.e. the index corresponds with the percentile value of the original measurements in relation to the site-specific cePDF. Colored (red-to-blue gradient) hexbins show the percentile CH₄ flux in the respective combined class, while white hexbins show the lack of measurements. The site FR-LAQ-I was not included for this analysis due to the presence of cattle in the flux footprint. (a) Aggregated CH₄ flux percentile values for each site, showing the median of each percentile flux within each aggregation unit. Black dots in hexbins indicate that the respective median percentile flux corresponds to CH₄ uptake, while the absence of black dots indicates CH₄ emission. The order of sites from left to right and from top to bottom follows the elevational gradient, with results for the highest site shown at the top left. (b) Aggregated CH₄ flux percentile values across all sites, calculated as the median of site-level hexbin values in (a), when data from at least two sites were

available for a specific combined class. Additional information on percentile distributions at each site is given in Table 2. See Table 1 for site name abbreviations.

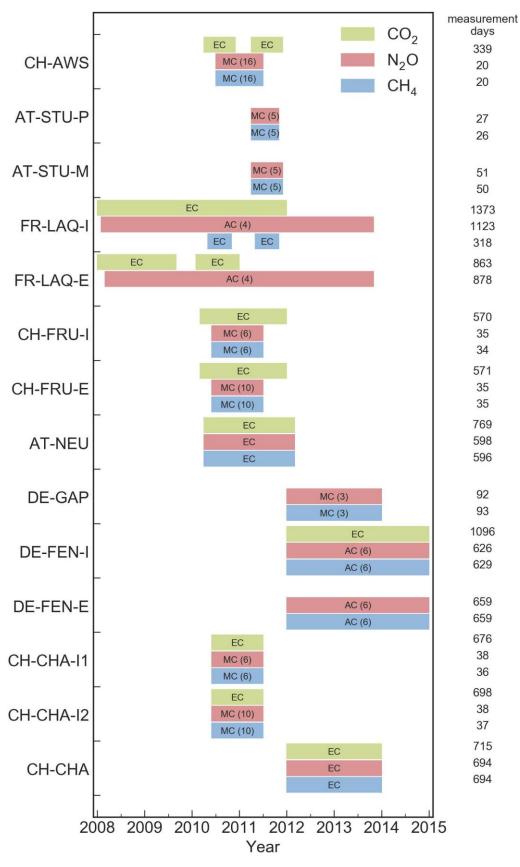
Figure 5 Linear regression analysis of average percentile fluxes across sites in classes of (a) soil temperature and (b) water-filled pore space, based on the respective hexbin classes shown in Figure 3b for N_2O fluxes and Figure 4b for CH_4 fluxes. The shaded area refers to the standard deviation of average percentile fluxes in the respective soil temperature or water-filled pore space class. Percentile distributions for each site along with percentile ranges across all sites in this analysis are given in Table 2.

Figure 6 Explained variance (r^2) from a multiple linear regression analysis of measured, nongapfilled, log-transformed N₂O daily average fluxes in dependence of soil temperature (TS) and water-filled pore space (WFPS), performed in a moving time window of 35 days. Results were calculated if a minimum of 13 days of data were available within a specific time window. Blue markers denote days with snow cover, vertical lines show management events (dotted: cutting, dashed: fertilization), grey horizontal bars show the regression time window for the respective r^2 . Red dots mark time periods where the regression was significant at P < 0.05. See Table 1 for site name abbreviations.

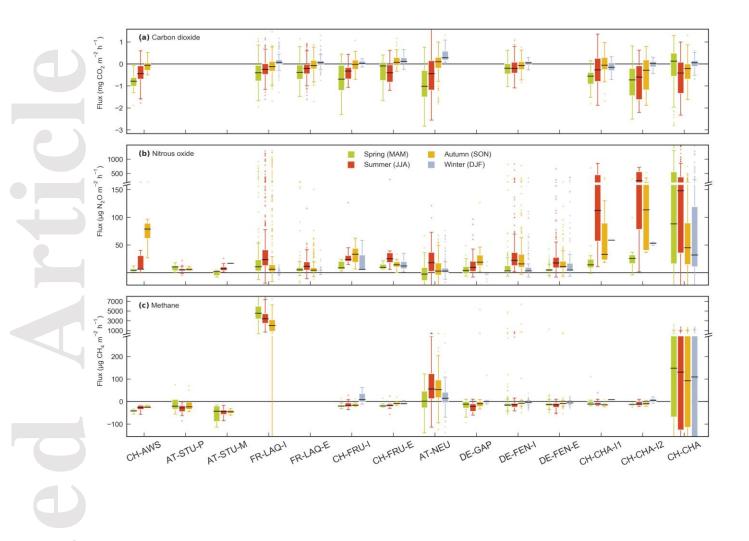
Figure 7 Explained variance (r^2) from a multiple linear regression analysis of measured, nongapfilled, log-transformed CH₄ daily average fluxes in dependence of soil temperature (TS) and water-filled pore space (WFPS), performed in a moving time window of 35 days. Results were calculated if a minimum of 13 days of data were available within a specific time window. Blue markers denote days with snow cover, vertical lines show management events (dotted: cutting, dashed: fertilization), grey horizontal bars show the regression time window for the respective r^2 . Red dots mark time periods where the regression was significant at P < 0.05. Note that no CH₄ measurements were available for FR-LAQ-E and that cattle were present in the flux footprint for CH₄ measurements at FR-LAQ-I. See Table 1 for site name abbreviations.

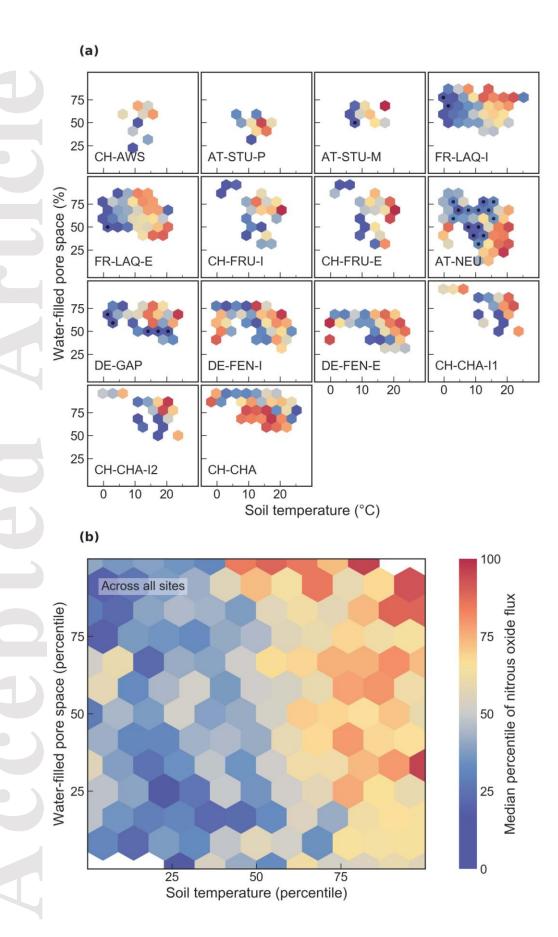
Figure 8 Measured, non-gapfilled N₂O fluxes at three sites during each fertilizer application of liquid slurry. Left panel: daily average fluxes for seven pre-fertilization days (-7 to -1), the day of application (0) and seven post-fertilization days (1 to 7), expressed in μ g m⁻² h⁻¹. Right panel: absolute ratio of measured fluxes to the 7-day pre-fertilization average for each management event. See Table 1 for site name abbreviations.

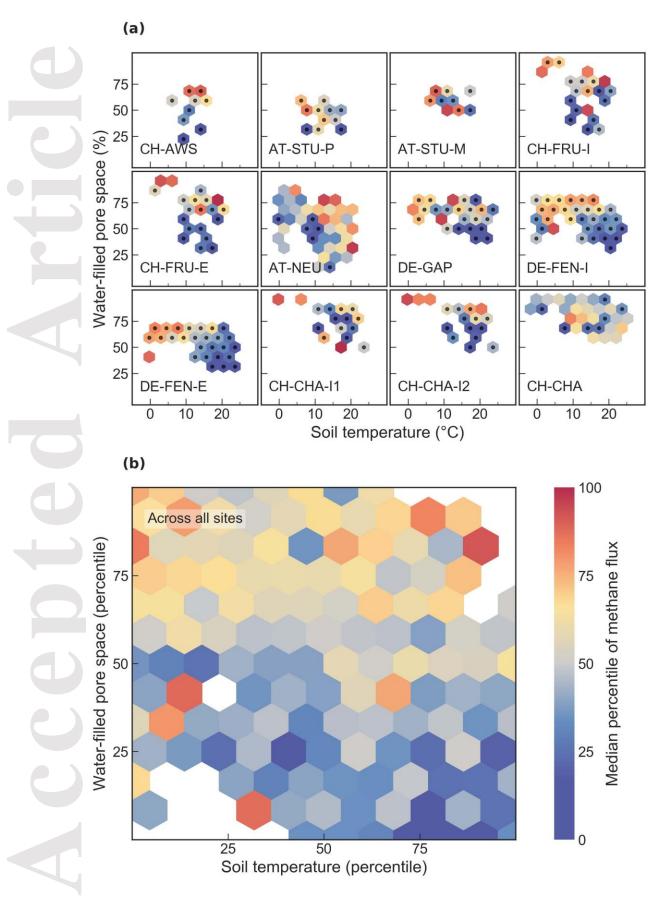
Figure 9 Measured, non-gapfilled CH₄ fluxes at three sites during each fertilizer application of liquid slurry. Left panel: daily average fluxes for seven pre-fertilization days (-7 to -1), the day of application (0) and seven post-fertilization days (1 to 7), expressed in μ g m⁻² h⁻¹. Right panel: absolute ratio of measured fluxes to the 7-day pre-fertilization average for each management event. See Table 1 for site name abbreviations.

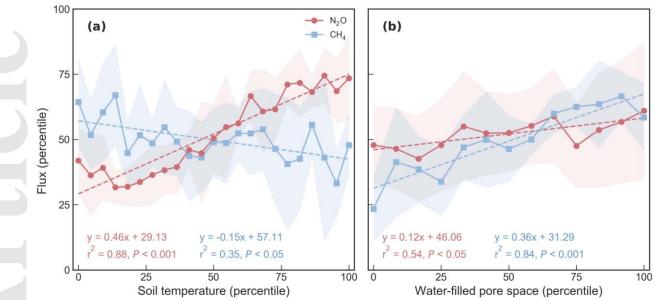


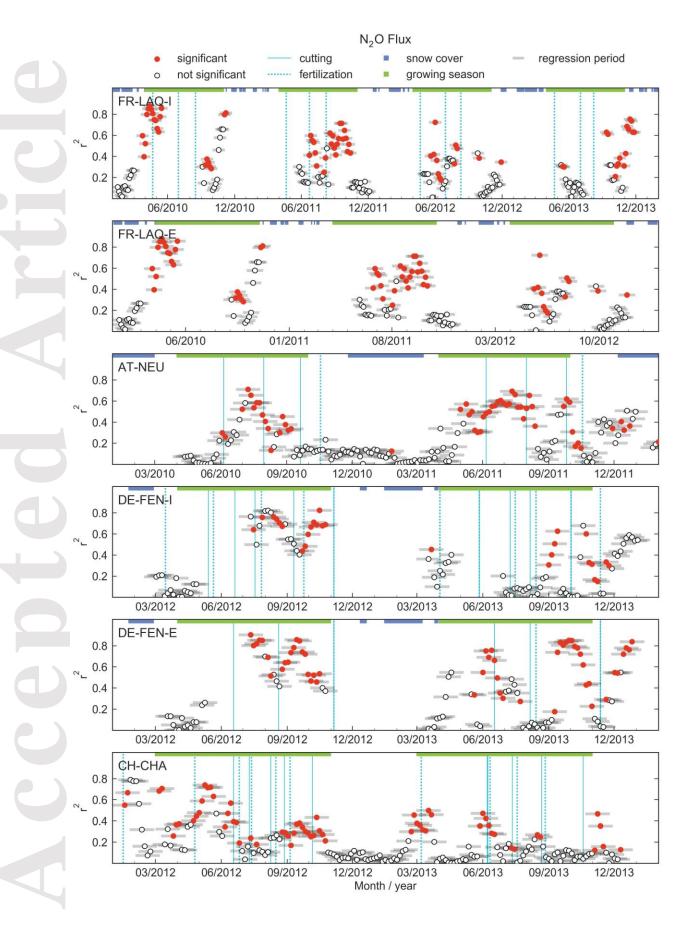
This article is protected by copyright. All rights reserved.



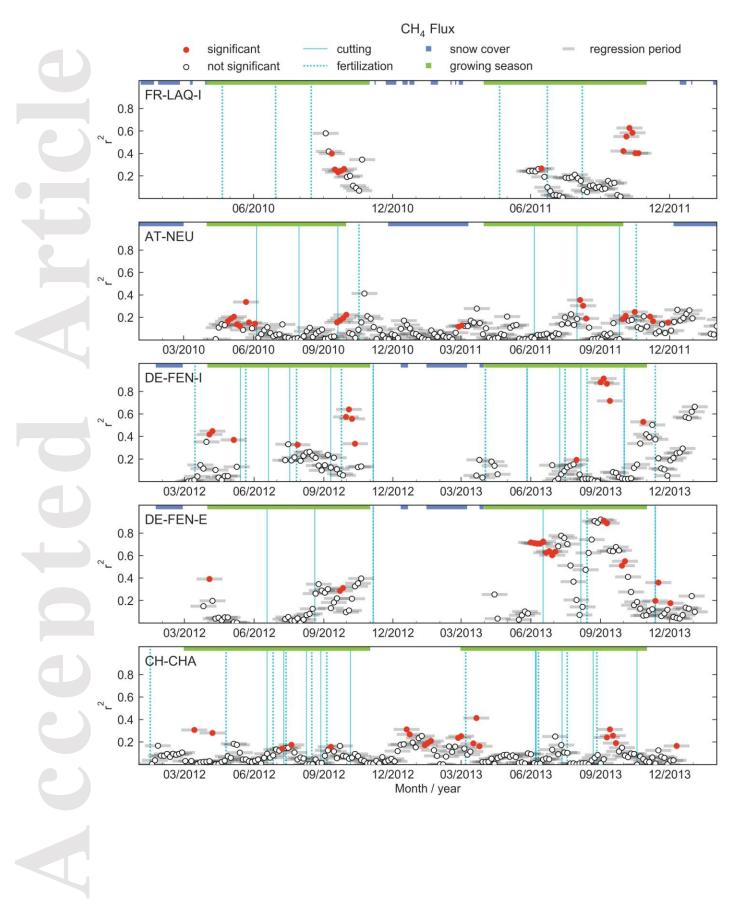








This article is protected by copyright. All rights reserved.



This article is protected by copyright. All rights reserved.

